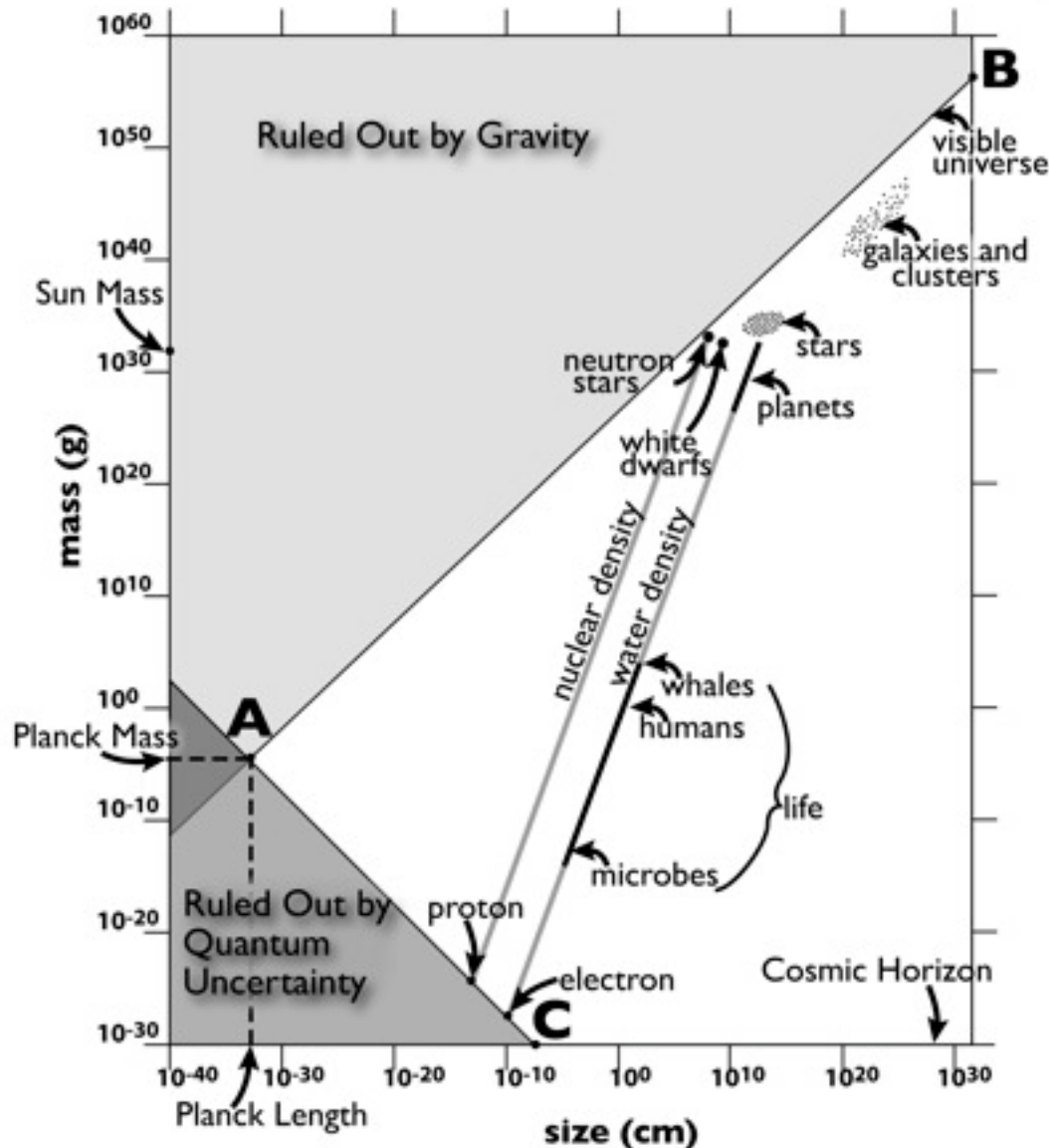# Physical Cosmology

Week 5

Big Bang Nucleosynthesis, Recombination, and Dark Matter Annihilation

Joel Primack

University of California, Santa Cruz

The Wedge of Material Reality

The **Planck Length**

$$l_{Pl} = \sqrt{\frac{hG}{2\pi c^3}} = 1.6 \times 10^{-33} \text{ cm}$$

is the smallest possible length. Here h is Planck's constant

$$h = 6.626068 \times 10^{-34} \text{ m}^2 \text{ kg} / \text{s}$$

The Planck Mass is

$$m_{Pl} = \sqrt{\frac{hc}{2\pi G}} = 2.2 \times 10^{-5} \text{ g}$$

The Compton (i.e. quantum) wavelength $l_C = \dfrac{h}{2\pi mc}$

equals the Schwarzschild radius $l_S \approx \dfrac{Gm}{c^2}$

when $m = m_{Pl} = 1.2 \times 10^{19} \text{ GeV/c}^2$

Big Bang Nucleosynthesis

BBN was conceived by Gamow in 1946 as an explanation for the formation of all the elements, but the absence of any stable nuclei with A=5,8 makes it impossible for BBN to proceed past Li. The formation of carbon and heavier elements occurs instead through the triple-α process in the centers of red giants (Burbidge[2], Fowler, & Hoyle 57). At the BBN baryon density of $2 \times 10^{-29} \, \Omega_b \, h^2 \, (T/T_0)^3$ g cm^{-3} $\approx 2 \times 10^{-5}$ g cm^{-3}, the probability of the triple-α process is negligible even though T $\approx 10^9$K.
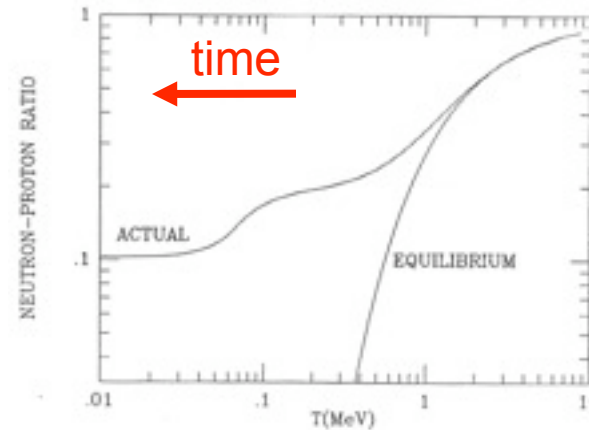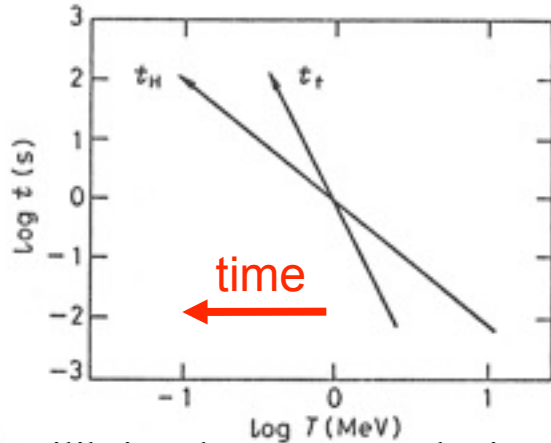
Kolb & Turner

Thermal equilibrium between n and p is maintained by weak interactions, which keeps n/p = exp(-Q/T) (where Q = m_n–m_p = 1.293 MeV) until about t $\approx$ 1 s. But because the neutrino mean free time $t_\nu^{-1} \approx \sigma_\nu \, n_{e\pm} \approx (G_F T)^2 (T^3)$ is increasing as $t_\nu \propto T^{-5}$ (here the Fermi constant $G_F \approx 10^{-5}$ GeV^{-2}), while the horizon size is increasing only as $t_H \approx (G\rho)^{-\frac{1}{2}} \approx M_{Pl} \, T^{-2}$, these interactions freeze out when T drops below about 0.8 MeV. This leaves n/(p+n) $\approx$ 0.14. The neutrons then decay with a mean lifetime 887 ± 2 s until they are mostly fused into D and then ^{4}He. The higher the baryon density, the higher the final abundance of ^{4}He and the lower the abundance of D that survives this fusion process. Since D/H is so sensitive to baryon density, David Schramm called deuterium the "baryometer." He and his colleagues also pointed out that since the horizon size increases more slowly with T^{-1} the larger the number of light neutrino species N_ν contributing to the energy density ρ, BBN predicted that $N_\nu \approx 3$ before N_ν was measured at accelerators by measuring the width of the Z^0 (Cyburt et al. 2005: 2.67<N_ν<3.85).

Neutrinos in the Early Universe
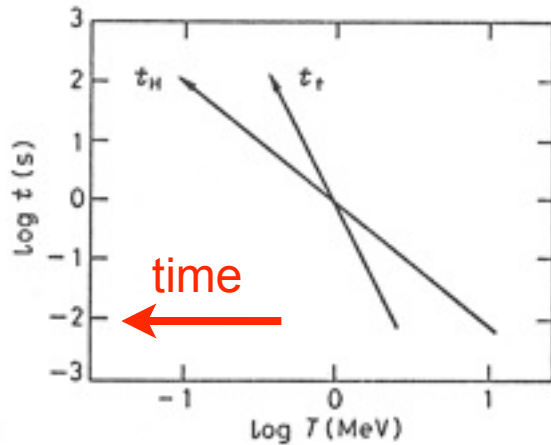
As we discussed, neutrino decoupling occurs at T ~ 1 MeV. After decoupling, the neutrino phase space distribution is

$f_\nu = [1+\exp(p_\nu c/T_\nu)]^{-1}$ $\big($ note: $\neq [1+\exp(E_\nu/T_\nu)]$

for NR neutrinos $\big)$

After e+e- annihilation, $T_\nu = (4/11)^{1/3} T_\gamma = 1.9K$. Proof :

Number densities of primordial particles

FermiDirac/BoseEinstein factor

$n_\gamma(T) = 2\,\zeta(3)\,\pi^{-2}\,T^3 = 400\ \text{cm}^{-3}\,(T/2.7K)^3$, $n_\nu(T) = (3/4)\,n_\gamma(T)$ including antineutrinos

Conservation of entropy s_I of interacting particles per comoving volume

$s_I = g_I(T)\,N_\gamma(T) = $ constant, where $N_\gamma = n_\gamma V$; we only include neutrinos for T>1 MeV.

Thus for T>1 MeV, $g_I = 2 + 4(7/8) + 6(7/8) = 43/4$ for γ, e+e-, and the three ν species, while for T< 1 MeV, $g_I = 2 + 4(7/8) = 11/2$. At e+e- annihilation, below about T=0.5 Mev, g_I drops to 2, so that $2N_{\gamma 0} = g_I(T<1\ \text{MeV})\,N_\gamma(T<1\ \text{MeV}) = (11/2)\,N_\gamma(T<1\ \text{MeV}) = (11/2)(4/3)\,N_\nu(T<1\ \text{MeV})$. Thus $n_{\nu 0} = (3/4)(4/11)\,n_{\gamma 0} = 109\ \text{cm}^{-3}\,(T/2.7K)^3$, or

$T_\nu = (4/11)^{1/3}\,T = 0.714\,T$

Statistical Thermodynamics

$$n_i = \frac{g_i}{2\pi^2}\left(\frac{kT_i}{\hbar c}\right)^3 I_i''(\pm), \quad \rho_i = \frac{g_i \, kT_i}{2\pi^2 c^2}\left(\frac{kT_i}{\hbar c}\right)^3 I_i^{21}(\pm), \quad \text{where}$$

$$I_i^{mn} \equiv \int_{\theta_i}^{\infty} x^m \left(x^2 - \theta_i^{-2}\right)^{n/2} \left(e^x \pm 1\right)^{-1} dx, \quad \theta_i = \frac{kT_i}{m_i c^2}, \quad g_i = \#\,\text{spin states}$$

+ Fermi-Dirac, - Bose-Einstein

$\theta_i \gg 1 \quad (ER): \quad I''(+) = \frac{3}{2}\zeta(3) = 1.803, \quad I^{21}(+) = 7\pi^4/120$

$$I''(-) = 2\zeta(3) = \frac{4}{3}I''(+), \quad I^{21}(-) = \pi^4/15 = \frac{8}{7}I^{21}(+)$$

$\theta_i \ll 1 \quad (NR): \quad n_i = \frac{\rho_i}{m_i} = \frac{g_i}{(2\pi)^{3/2}}\left(\frac{kT_i}{\hbar c}\right)^3 \theta_i^{-3/2} e^{-\theta_i^{-1}} \quad (\underline{\text{not}} \; \nu\text{'s})$

$$\left[\text{Note: } \zeta(3) = 1.2020569\cdots = \sum_{k=1}^{\infty}\frac{1}{k^3} = \prod_{\text{primes}}\left(1 - p^{-3}\right)^{-1}!\right]$$

Statistical Thermodynamics

$$n_i = \frac{g_i}{2\pi^2}\left(\frac{kT_i}{\hbar c}\right)^3 I_i''(\pm), \quad \rho_i = \frac{g_i \, kT_i}{2\pi^2 c^2}\left(\frac{kT_i}{\hbar c}\right)^3 I_i^{21}(\pm), \quad \text{where}$$

$$I_i^{mn} \equiv \int_{\theta_i}^{\infty} x^m \left(x^2 - \theta_i^{-2}\right)^{n/2} \left(e^x \pm 1\right)^{-1} dx, \quad \theta_i = \frac{kT_i}{m_i c^2}, \quad g_i = \#\text{ spin states}$$

+ Fermi-Dirac, - Bose-Einstein

$\theta_i \gg 1$ (ER): $\quad I''(+) = \frac{3}{2}\zeta(3) = 1.803, \quad I^{21}(+) = 7\pi^4/120$

$\quad\quad\quad\quad\quad\quad I''(-) = 2\zeta(3) = \frac{4}{3}I''(+), \quad I^{21}(-) = \pi^4/15 = \frac{8}{7}I^{21}(+)$

$\theta_i \ll 1$ (NR): $\quad n_i = \frac{\rho_i}{m_i} = \frac{g_i}{(2\pi)^{3/2}}\left(\frac{kT_i}{\hbar c}\right)^3 \theta_i^{-3/2} e^{-\theta_i^{-1}} \quad (\text{not } \nu\text{'s})$

$$\left[\text{Note: } \zeta(3) = 1.2020569\cdots = \sum_{k=1}^{\infty}\frac{1}{k^3} = \prod_{\text{primes}}\left(1 - p^{-3}\right)^{-1}\right]$$

Boltzmann Equation

$$a^{-3}\frac{d\left(n_1 a^3\right)}{dt} = \int \frac{d^3p_1}{(2\pi)^3 2E_1} \int \frac{d^3p_2}{(2\pi)^3 2E_2} \int \frac{d^3p_3}{(2\pi)^3 2E_3} \int \frac{d^3p_4}{(2\pi)^3 2E_4}$$

Dodelson (3.1)

$$\times (2\pi)^4 \delta^3(p_1 + p_2 - p_3 - p_4)\delta(E_1 + E_2 - E_3 - E_4)|\mathcal{M}|^2$$

$$\times \{f_3 f_4[1 \pm f_1][1 \pm f_2] - f_1 f_2[1 \pm f_3][1 \pm f_4]\}.$$

+ bosons
- fermions

In the absence of interactions (rhs=0) n_1 falls as a^{-3}

We will typically be interested in T>> E-μ (where μ is the chemical potential). In this limit, the exponential in the Fermi-Dirac or Bose-Einstein distributions is much larger than the ±1 in the denominator, so that

$$f(E) \rightarrow e^{\mu/T} e^{-E/T}$$

and the last line of the Boltzmann equation above simplifies to

$$f_3 f_4[1 \pm f_1][1 \pm f_2] - f_1 f_2[1 \pm f_3][1 \pm f_4]$$

$$\rightarrow \quad e^{-(E_1+E_2)/T}\left\{e^{(\mu_3+\mu_4)/T} - e^{(\mu_1+\mu_2)/T}\right\}.$$

The number densities are given by $n_i = g_i e^{\mu_i/T} \int \frac{d^3p}{(2\pi)^3} e^{-E_i/T}$. For our applications, i's are

Table 3.1. Reactions in This Chapter: $1 + 2 \leftrightarrow 3 + 4$

	1	2	3	4
Neutron-Proton Ratio	n	ν_e or e^+	p	e^- or $\bar{\nu}_e$
Recombination	e	p	H	γ
Dark Matter Production	X	X	l	l

$$n_i^{(0)} \equiv g_i \int \frac{d^3 p}{(2\pi)^3} e^{-E_i/T} = \begin{cases} g_i \left(\frac{m_i T}{2\pi}\right)^{3/2} e^{-m_i/T} & m_i \gg T \\ g_i \frac{T^3}{\pi^2} & m_i \ll T \end{cases}. \qquad (3.6)$$

With this defintion, $e^{\mu_i/T}$ can be rewritten as $n_i/n_i^{(0)}$, so the last line of Eq. (3.1) is equal to

$$e^{-(E_1+E_2)/T} \left\{ \frac{n_3 n_4}{n_3^{(0)} n_4^{(0)}} - \frac{n_1 n_2}{n_1^{(0)} n_2^{(0)}} \right\}. \qquad (3.7)$$

With these approximations the Boltzmann equation now simplifies enormously. Define the thermally averaged cross section as

$$\langle \sigma v \rangle \equiv \frac{1}{n_1^{(0)} n_2^{(0)}} \int \frac{d^3 p_1}{(2\pi)^3 2E_1} \int \frac{d^3 p_2}{(2\pi)^3 2E_2} \int \frac{d^3 p_3}{(2\pi)^3 2E_3} \int \frac{d^3 p_4}{(2\pi)^3 2E_4} e^{-(E_1+E_2)/T}$$

$$\times (2\pi)^4 \delta^3(p_1 + p_2 - p_3 - p_4) \delta(E_1 + E_2 - E_3 - E_4) |\mathcal{M}|^2. \qquad (3.8)$$

Then, the Boltzmann equation becomes

$$a^{-3} \frac{d\left(n_1 a^3\right)}{dt} = n_1^{(0)} n_2^{(0)} \langle \sigma v \rangle \left\{ \frac{n_3 n_4}{n_3^{(0)} n_4^{(0)}} - \frac{n_1 n_2}{n_1^{(0)} n_2^{(0)}} \right\}. \qquad (3.9)$$

If the reaction rate $n_2 \langle \sigma v \rangle$ is much smaller than the expansion rate (~ H), then the {} on the rhs must vanish. This is called *chemical equilibrium* in the context of the early universe, *nuclear statistical equilibrium* (NSE) in the context of Big Bang nucleosynthesis, and the *Saha equation* when discussing recombination of electrons and protons to form neutral hydrogen.

As the temperature of the universe cools to 1 MeV, the cosmic plasma consists of:

- **Relativistic particles in equilibrium: photons, electrons and positrons.** These are kept in close contact with each other by electromagnetic interactions such as $e^+ e^- \leftrightarrow \gamma\gamma$. Besides a small difference due to fermion/boson statistics, these all have the same abundances.

- **Decoupled relativistic particles: neutrinos.** At temperatures a little above 1 MeV, the rate for processes such as $\nu e \leftrightarrow \nu e$ which keep neutrinos coupled to the rest of the plasma drops beneath the expansion rate. Neutrinos therefore share the same temperature as the other relativistic particles, and hence are roughly as abundant, but they do not couple to them.

- **Nonrelativistic particles: baryons.** If there had been no asymmetry in the initial number of baryons and anti-baryons, then both would be completely depleted by 1 MeV. However, such an asymmetry did exist: $(n_b - n_{\bar{b}})/s \sim 10^{-10}$ initially,[1] and this ratio remains constant throughout the expansion. By the time the temperature is of order 1 MeV, all anti-baryons have annihilated away (Exercise 12) so

$$\eta_b \equiv \frac{n_b}{n_\gamma} = 5.5 \times 10^{-10} \left(\frac{\Omega_b h^2}{0.020} \right). \tag{3.11}$$

There are thus many fewer baryons than relativistic particles when $T \sim$ MeV.

Binding Energy per Nucleon
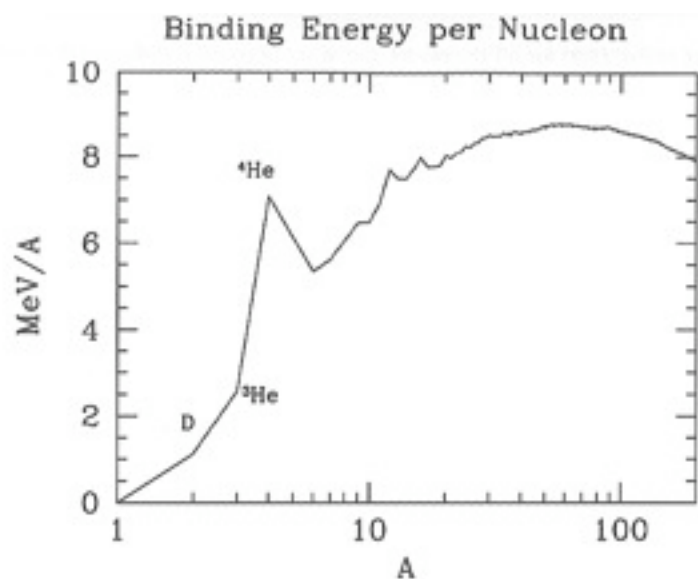
Figure 3.1. Binding energy of nuclei as a function of mass number. Iron has the highest binding energy, but among the light elements, ^{4}He is a crucial local maximum. Nucleosynthesis in the early universe essentially stops at ^{4}He because of the lack of tightly bound isotopes at $A = 5 - 8$. In the high-density environment of stars, three ^{4}He nuclei fuse to form ^{12}C, but the low baryon number precludes this process in the early universe.

Lightning Introduction to Nuclear Physics

A single proton is a hydrogen nucleus, referred to as ^{1}H or simply p; a proton and a neutron make up deuterium, ^{2}H or D; one proton and two neutrons make tritium, ^{3}H or T. Nuclei with two protons are helium; these can have one neutron (^{3}He) or two (^{4}He). Thus unique elements have a fixed number of protons, and isotopes of a given element have differing numbers of neutrons. The total number of neutrons and protons in the nucleus, the *atomic number*, is a superscript before the name of the element.

The total mass of a nucleus with Z protons and $A - Z$ neutrons differs slightly from the mass of the individual protons and neutrons alone. This difference is called the binding energy, defined as

$$B \equiv Z m_p + (A - Z) m_n - m \tag{3.12}$$

where m is the mass of the nucleus. For example, the mass of deuterium is 1875.62 MeV while the sum of the neutron and proton masses is 1877.84 MeV, so the binding energy of deuterium is 2.22 MeV. Nuclear binding energies are typically in the MeV range, which explains why Big Bang nucleosynthesis occurs at temperatures a bit less than 1 MeV even though nuclear masses are in the GeV range.

Neutrons and protons can interconvert via weak interactions:

$$p + \bar{\nu} \leftrightarrow n + e^+ \quad ; \quad p + e^- \leftrightarrow n + \nu \quad ; \quad n \leftrightarrow p + e^- + \bar{\nu} \tag{3.13}$$

where all the reactions can proceed in either direction. The light elements are built up via electromagnetic interactions. For example, deuterium forms from $p + n \rightarrow D + \gamma$. Then, $D + D \rightarrow n + {}^3$He, after which ^{3}He$+$D $\rightarrow p + {}^4$He produces ^{4}He.

$$\frac{n_D}{n_n n_p} = \frac{n_D^{(0)}}{n_n^{(0)} n_p^{(0)}}. \tag{3.14}$$

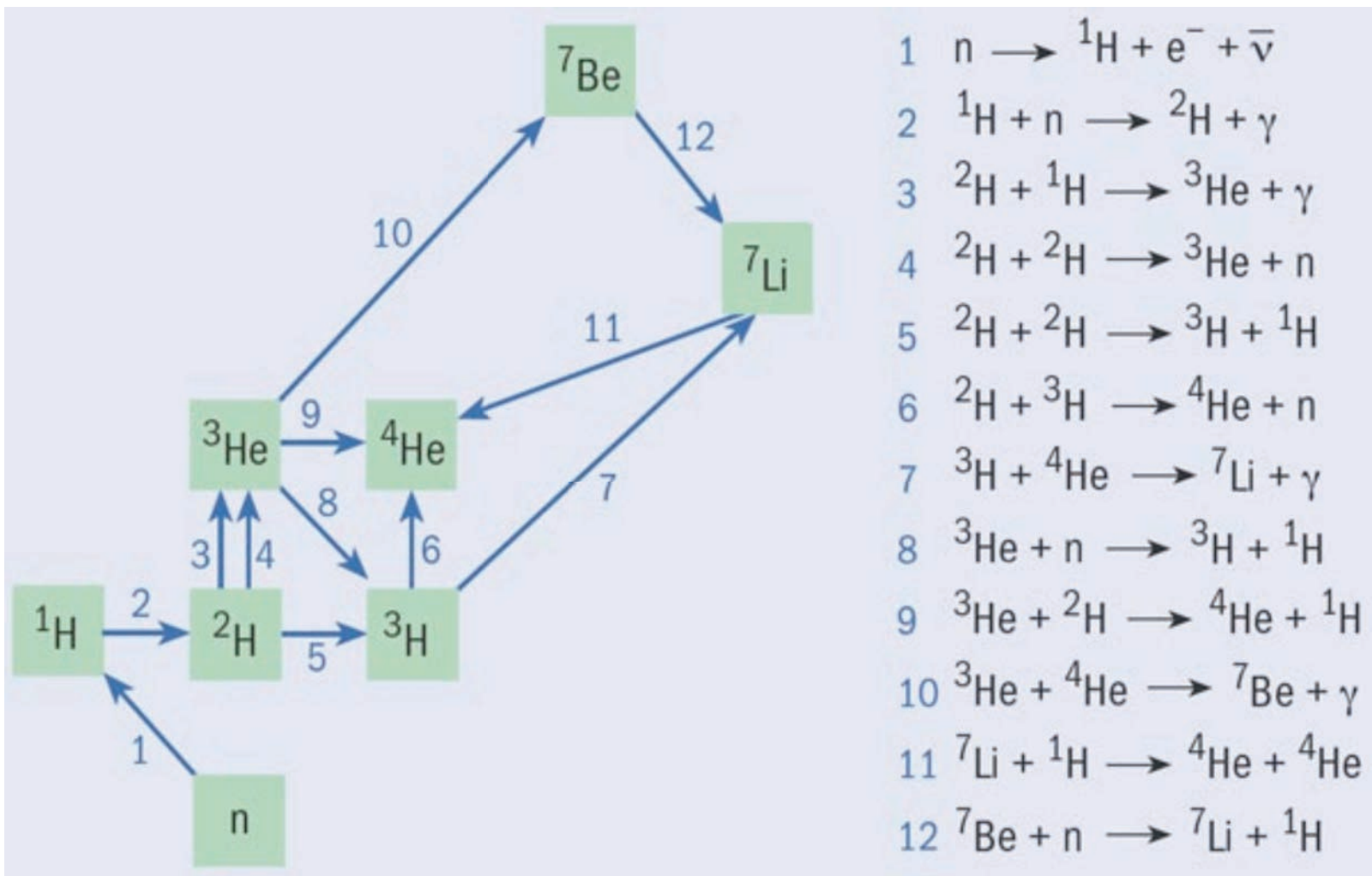The integrals on the right, as given in Eq. (3.6), lead to

$$\frac{n_D}{n_n n_p} = \frac{3}{4} \left(\frac{2\pi m_D}{m_n m_p T} \right)^{3/2} e^{[m_n + m_p - m_D]/T}, \tag{3.15}$$

the factor of 3/4 being due to the number of spin states (3 for D and 2 each for p and n). In the prefactor, m_D can be set to $2m_n = 2m_p$, but in the exponential the small difference between $m_n + m_p$ and m_D is important: indeed the argument of the exponential is by definition equal to the binding energy of deuterium, $B_D = 2.22$ MeV. Therefore, as long as equilibrium holds,

$$\frac{n_D}{n_n n_p} = \frac{3}{4} \left(\frac{4\pi}{m_p T} \right)^{3/2} e^{B_D/T}. \tag{3.16}$$

Both the neutron and proton density are proportional to the baryon density, so roughly,

$$\frac{n_D}{n_b} \sim \eta_b \left(\frac{T}{m_p} \right)^{3/2} e^{B_D/T}. \tag{3.17}$$

The diagram shows nuclear reactions with the following legend:

1. $n \longrightarrow {}^{1}H + e^- + \bar{\nu}$
2. ${}^{1}H + n \longrightarrow {}^{2}H + \gamma$
3. ${}^{2}H + {}^{1}H \longrightarrow {}^{3}He + \gamma$
4. ${}^{2}H + {}^{2}H \longrightarrow {}^{3}He + n$
5. ${}^{2}H + {}^{2}H \longrightarrow {}^{3}H + {}^{1}H$
6. ${}^{2}H + {}^{3}H \longrightarrow {}^{4}He + n$
7. ${}^{3}H + {}^{4}He \longrightarrow {}^{7}Li + \gamma$
8. ${}^{3}He + n \longrightarrow {}^{3}H + {}^{1}H$
9. ${}^{3}He + {}^{2}H \longrightarrow {}^{4}He + {}^{1}H$
10. ${}^{3}He + {}^{4}He \longrightarrow {}^{7}Be + \gamma$
11. ${}^{7}Li + {}^{1}H \longrightarrow {}^{4}He + {}^{4}He$
12. ${}^{7}Be + n \longrightarrow {}^{7}Li + {}^{1}H$

Deuterium nuclei (^{2}H) were produced by collisions between protons and neutrons, and further nuclear collisions led to every neutron grabbing a proton to form the most tightly bound type of light nucleus: ^{4}He. This process was complete after about five minutes, when the universe became too cold for nuclear reactions to continue. Tiny amounts of deuterium, ^{3}He, ^{7}Li, and ^{7}Be were produced as by-products, with the ^{7}Be undergoing beta decay to form ^{7}Li. Almost all of the protons that were not incorporated into ^{4}He nuclei remained as free particles, and this is why the universe is close to 25% ^{4}He and 75% H by mass. The other nuclei are less abundant by several orders of magnitude.
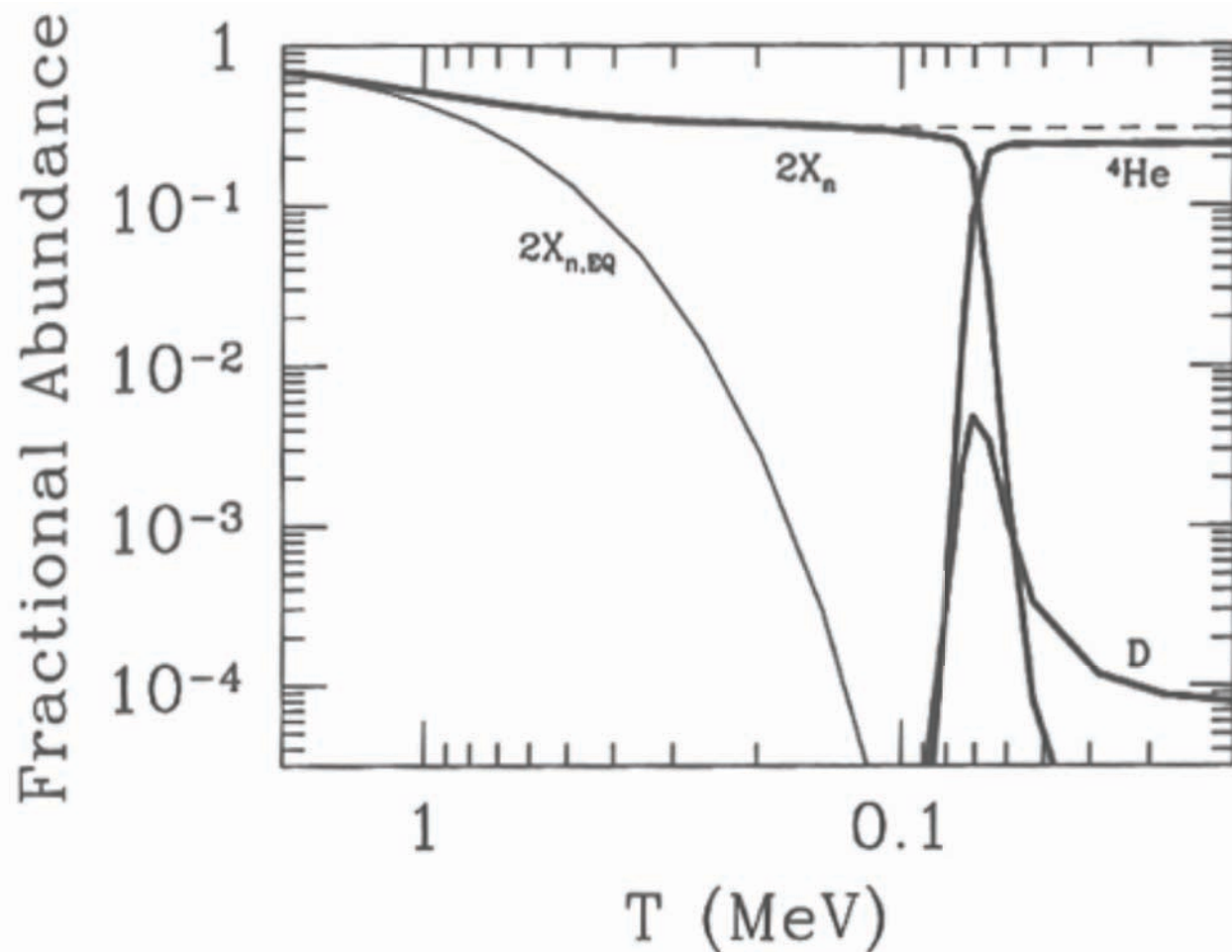
Figure 3.2. Evolution of light element abundances in the early universe. Heavy solid curves are results from Wagoner (1973) code; dashed curve is from integration of Eq. (3.27); light solid curve is twice the neutron equilibrium abundance. Note the good agreement of Eq. (3.27) and the exact result until the onset of neutron decay. Also note that the neutron abundance falls out of equilibrium at $T \sim$ MeV.
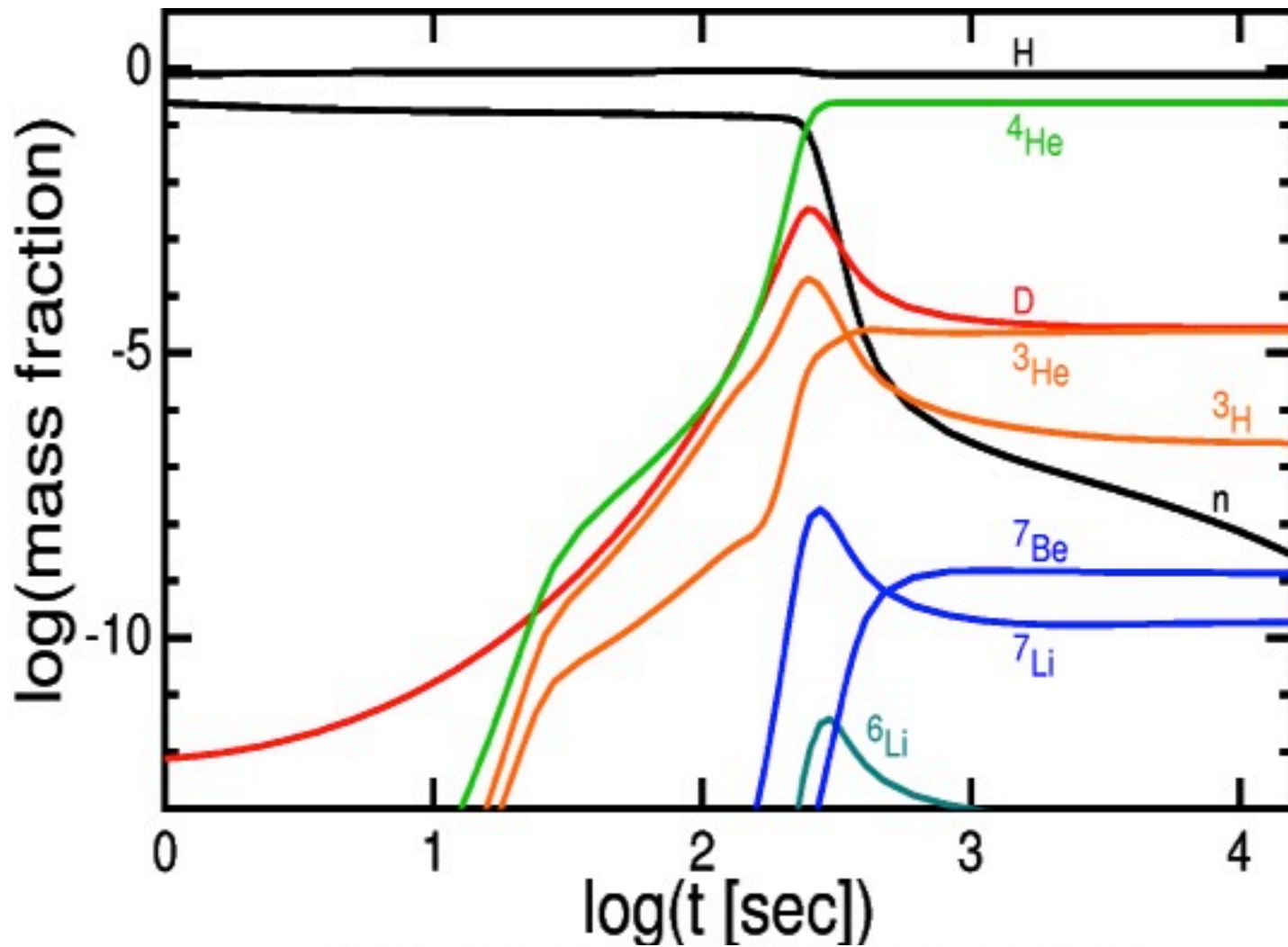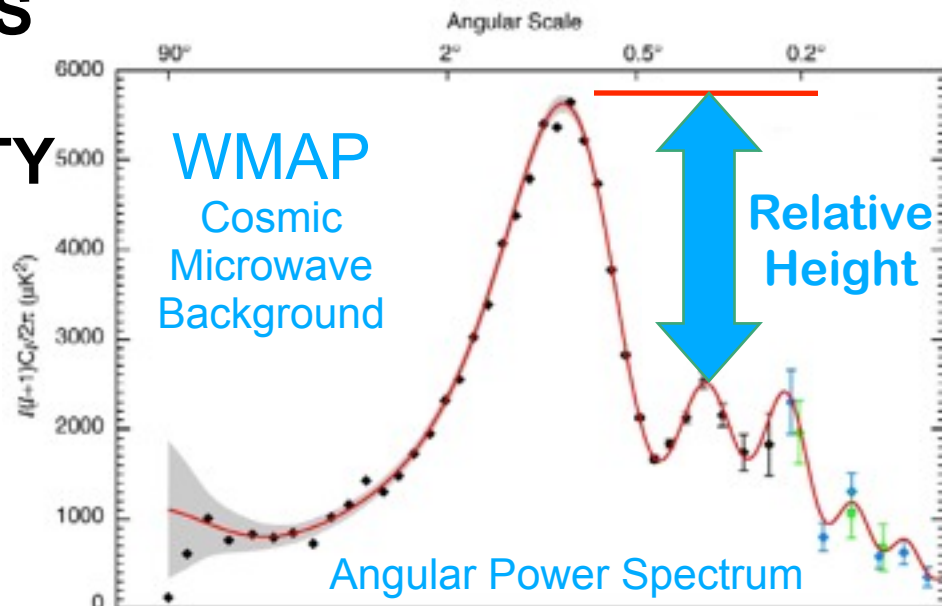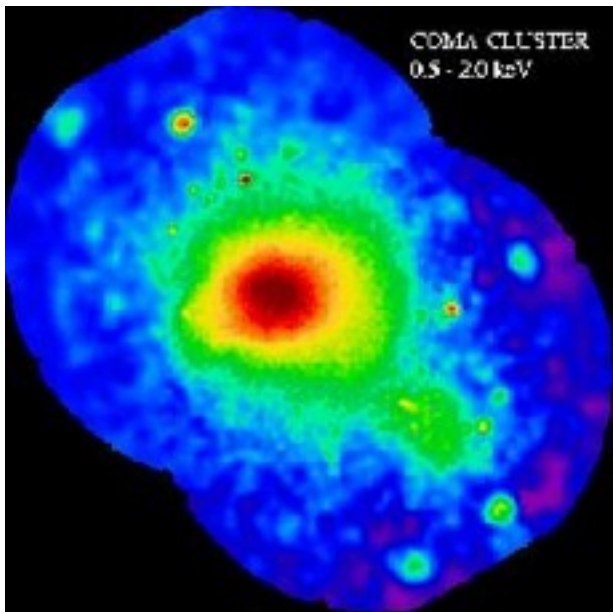
The detailed production of the lightest elements out of protons and neutrons during the first three minutes of the universe's history. The nuclear reactions occur rapidly when the temperature falls below a billion degrees Kelvin. Subsequently, the reactions are shut down, because of the rapidly falling temperature and density of matter in the expanding universe.

Ken Kawano's (1992) BBN code is available at
http://www-thphys.physics.ox.ac.uk/users/SubirSarkar/bbn.html

5 INDEPENDENT MEASURES AGREE: ATOMS ARE ONLY 4% OF THE COSMIC DENSITY

Galaxy Cluster in X-rays

COMA CLUSTER
0.5 - 2.0 keV

WMAP
Cosmic Microwave Background

Relative Height

Angular Scale

$l(l+1)C_l/2\pi$ (μK^2)

Angular Power Spectrum

Deuterium Abundance + Big Bang Nucleosynthesis

Number Fraction $\times 10^{-5}$

D

^{3}He

WMAP

Baryon Density $\Omega_b h^2$
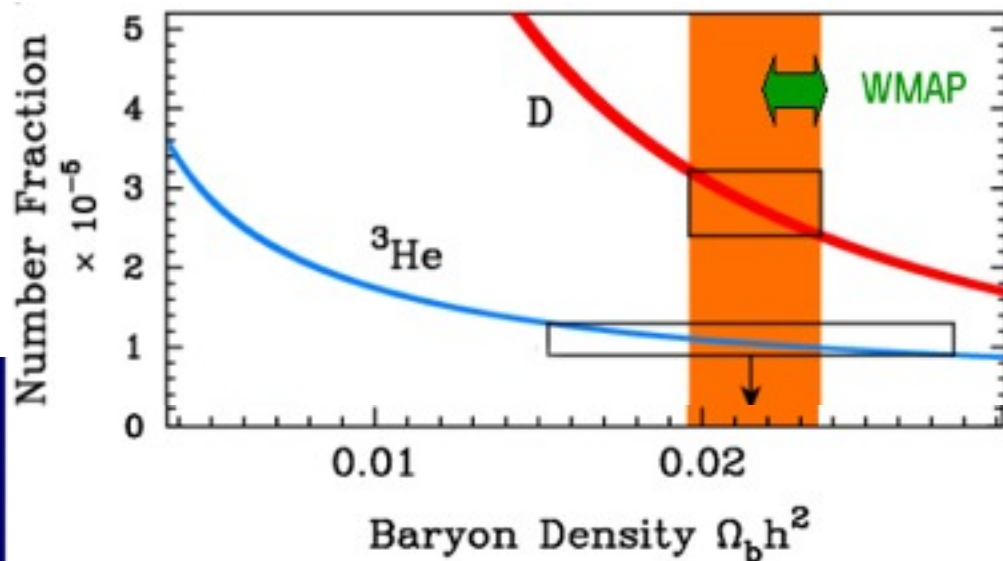
Absorption of Quasar Light

Q1422+2309 z=3.62

Intensity

Emitted wavelength, Å
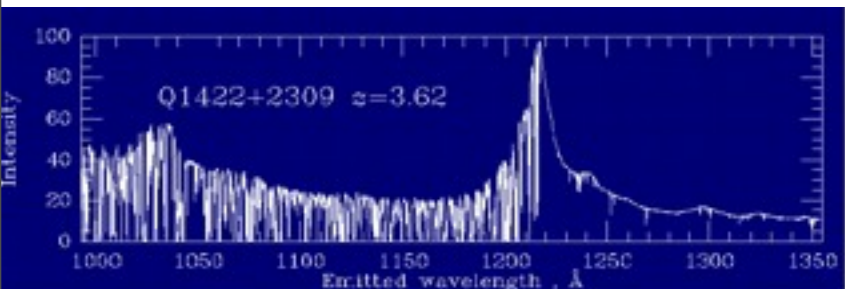
& BAO WIGGLES IN GALAXY P(k)

BAO WIGGLES IN GALAXY P(k)

Sound waves that propagate in the opaque early universe imprint a characteristic scale in the clustering of matter, providing a "standard ruler" whose length can be computed using straightforward physics and parameters that are tightly constrained by CMB observations. Measuring the angle subtended by this scale determines a distance to that redshift and constrains the expansion rate.

The detection of the acoustic oscillation scale is one of the key accomplishments of the SDSS, and even this moderate signal-to-noise measurement substantially tightens constraints on cosmological parameters. Observing the evolution of the BAO standard ruler provides one of the best ways to measure whether the dark energy parameters changed in the past.

M. White lectures 08

BAO WIGGLES IN GALAXY P(k)

CMB

SDSS Galaxy P(k)

W. Percival 06

SDSS Galaxy ξ(k)

D. Eisenstein+05

$\Omega_m h^2$	$\Omega_m h^2$	
0.12	0.024	
0.13	0.024	
0.14	0.024	
0.105	0.0	Pure ΛCDM
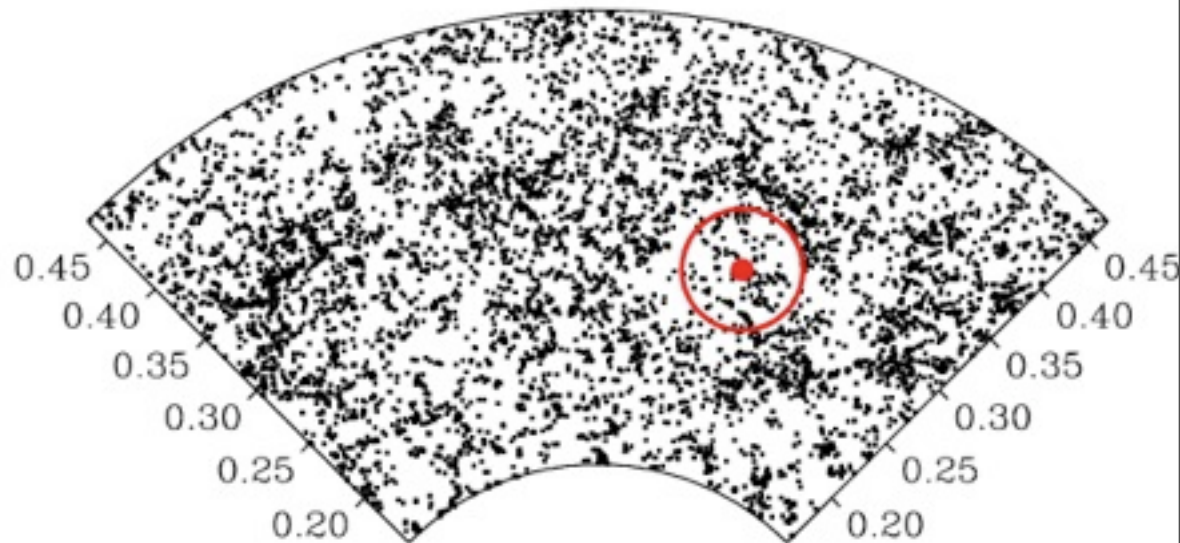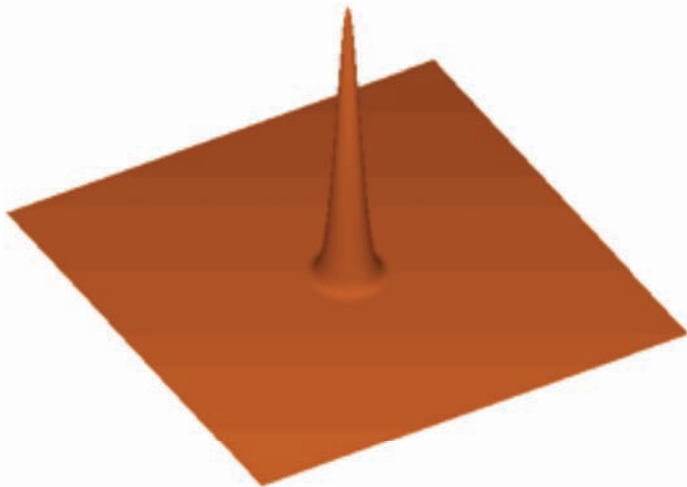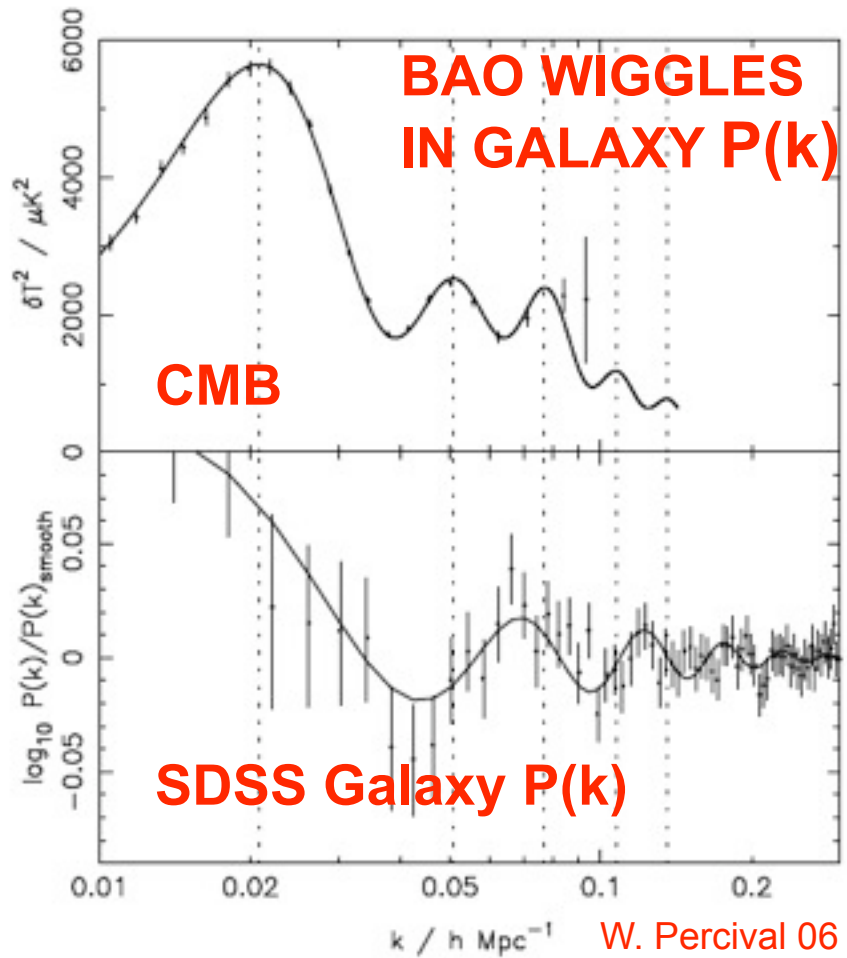
Fig. 3. Upper panel: The TT power spectrum recovered from the 3-year WMAP data (Hinshaw et al. 2006), projected into comoving space assuming a cosmological model with $\Omega_m = 0.25$ and $\Omega_V = 0.75$. For comparison, in the lower panel we plot the baryon oscillations calculated by dividing the SDSS power spectrum with a smooth cubic spline fit (Percival et al. 2007a). Vertical dotted lines show the positions of the peaks in the CMB power spectrum. As can be seen, there is still a long way to go before low redshift observations can rival the CMB in terms of the significance of the acoustic oscillation signal.

 All Visible Matter

All Other Visible Atoms

Hydrogen and Helium

Novus Ordo Seclorum

stars

Periodic Table

White - Big Bang   Pink - Cosmic Rays
Yellow - Small Stars   Green - Large Stars
Blue - Supernovae

VISIBLE MATTER

ALL OTHER VISIBLE ATOMS

HYDROGEN AND HELIUM

NOVUS ORDO SECLORUM

stardust

stars

COSMIC DENSITY PYRAMID

ALL MATTER AND ENERGY

All Other Visible Atoms 0.01%

Hydrogen and Helium 0.5%

Invisible Atoms 4%

Cold Dark Matter 25%

Dark Energy 70%

NEW ORDER OF THE UNIVERSE

BBN Predicted vs. Measured Abundances of D, ³He, ⁴He, and ⁷Li

BBN Predicted vs. Measured Abundances of D, ^{3}He, ^{4}He, and ^{7}Li

^{7}Li IS NOW DISCORDANT unless stellar diffusion destroys ^{7}Li

Baryon to Photon Ratio $\eta \times 10^{-10}$
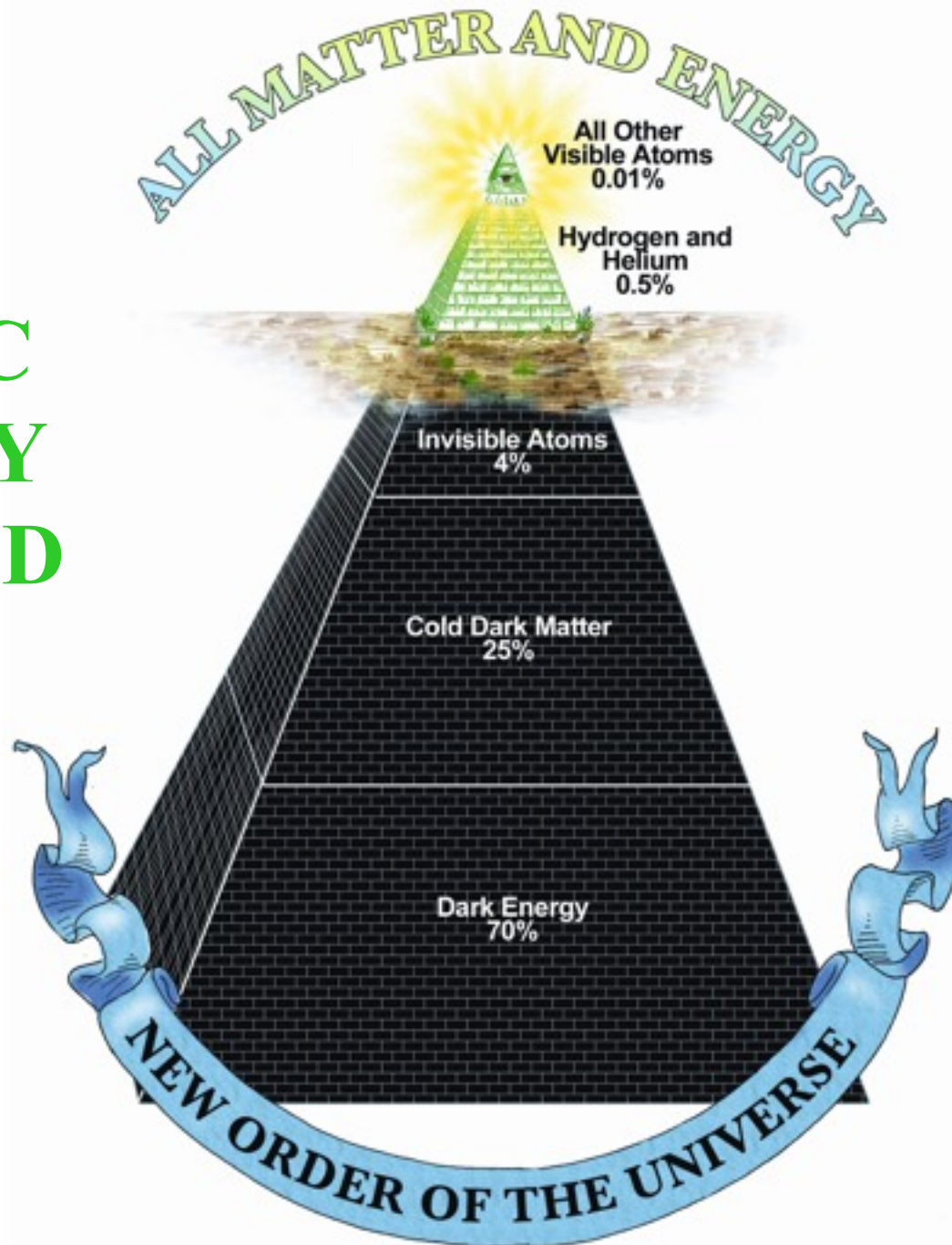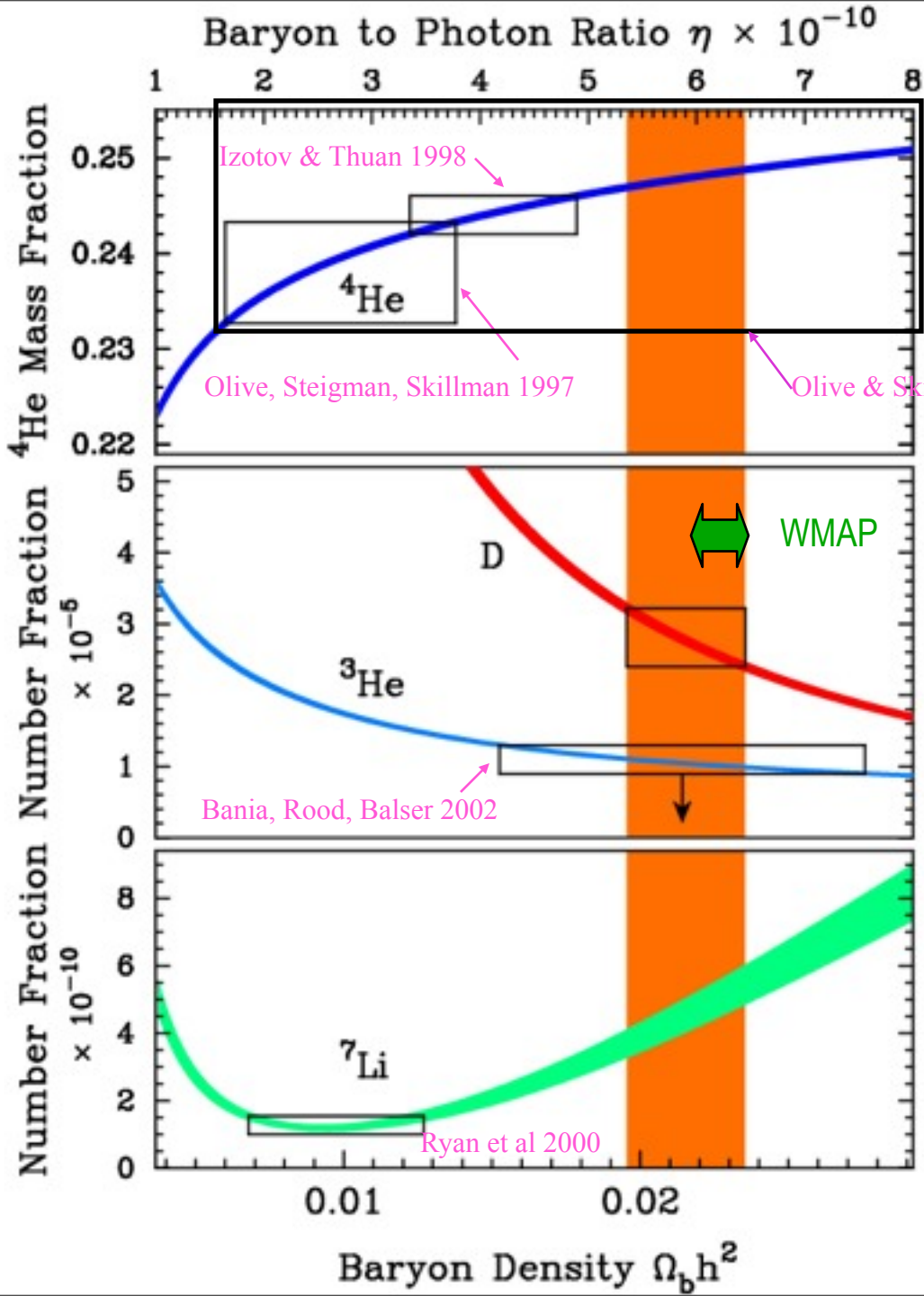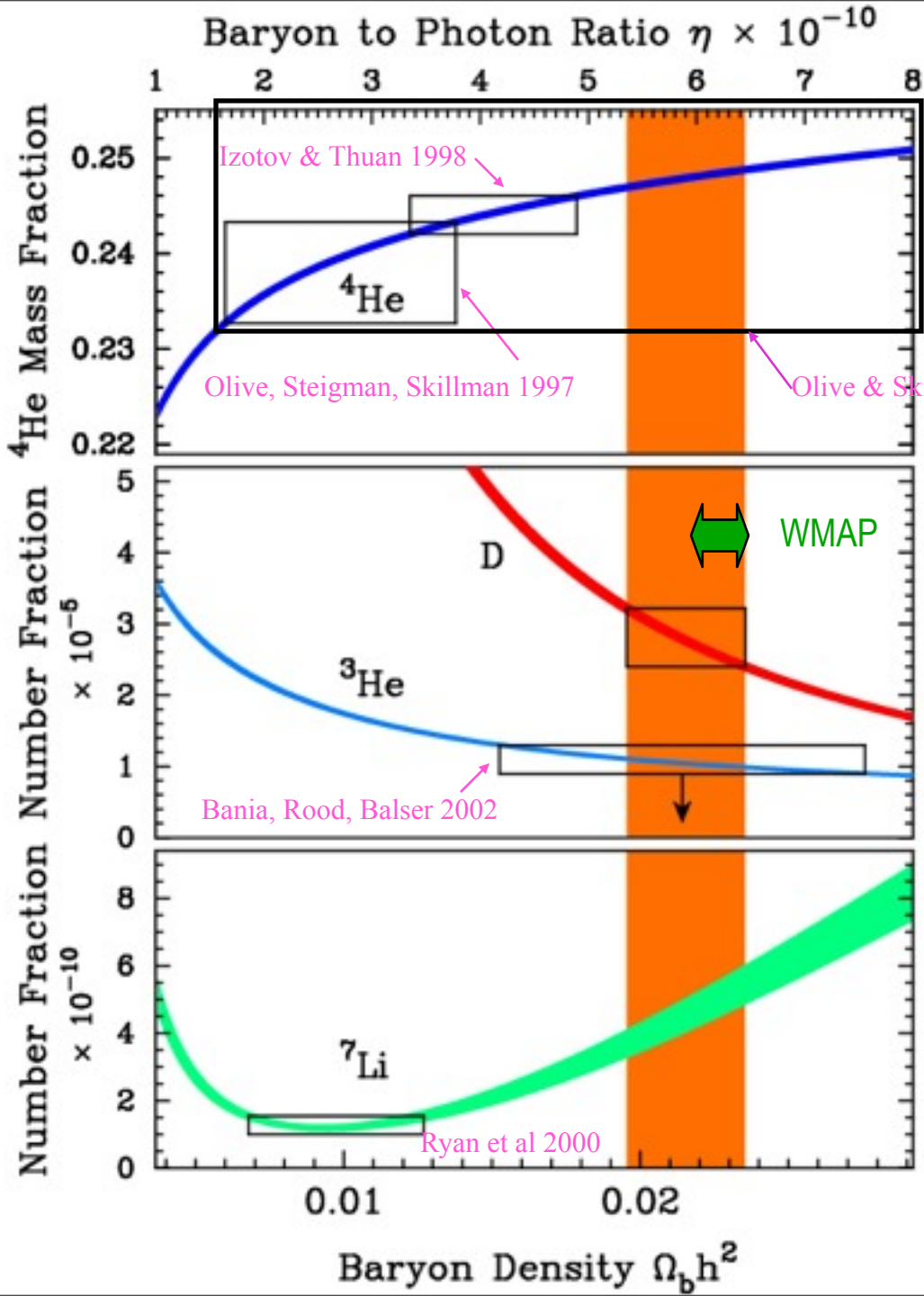
Izotov & Thuan 1998

Izotov & Thuan 2004: $\Omega_b h^2 = 0.012 \pm 0.0025$

Olive, Steigman, Skillman 1997

^{4}He

Olive & Skillman 2004: **big uncertainties**

D

WMAP

WMAP (Spergel et al. 2003) says that $\Omega_b h^2 = 0.0224 \pm 0.0009$ (with their running spectral index model)

^{3}He

Bania, Rood, Balser 2002

BBN predictions are from Burles, Nollett, & Turner 2001

^{7}Li

Ryan et al 2000

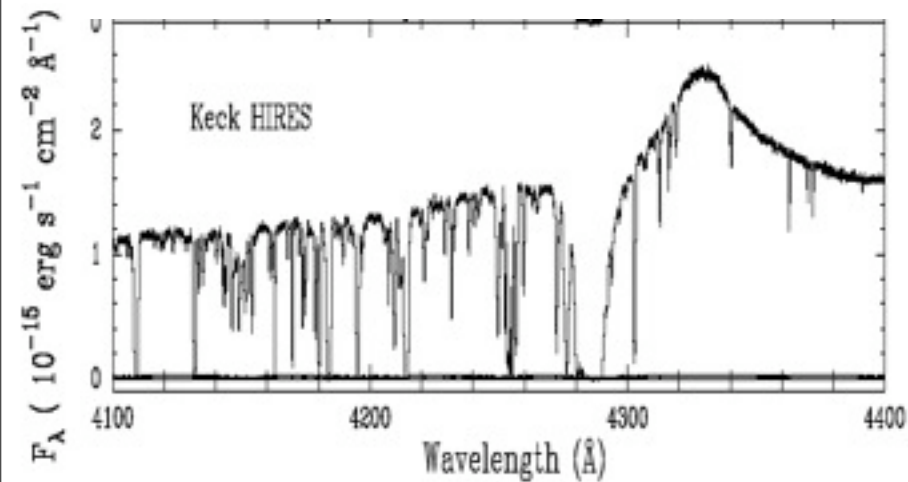D/H is from Kirkman, Tytler, Suzuki, O'Meara, & Lubin 2004, giving $\Omega_b h^2 = 0.0214 \pm 0.0020$

Baryon Density $\Omega_b h^2$

Deuterium absorption at redshift 2.525659 towards Q1243+3047

Keck HIRES

The Lyα absorption near 4285 Å is from the system in which we measure D/H.

The detection of Deuterium and the modeling of this system seem convincing. This is just a portion of the evidence that the Tytler group presented in this paper. They have similarly convincing evidence for several other Lyman alpha clouds in quasar spectra.
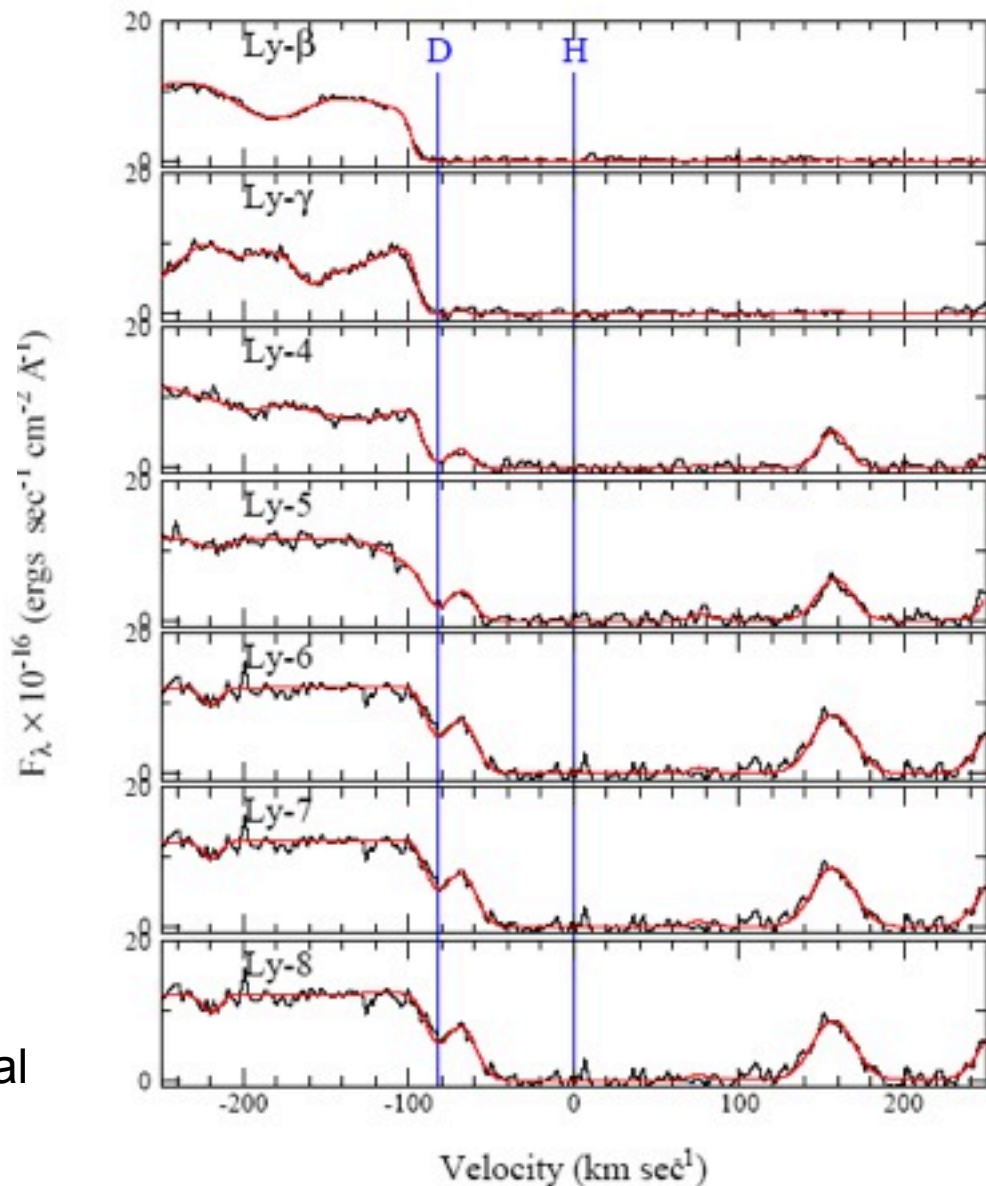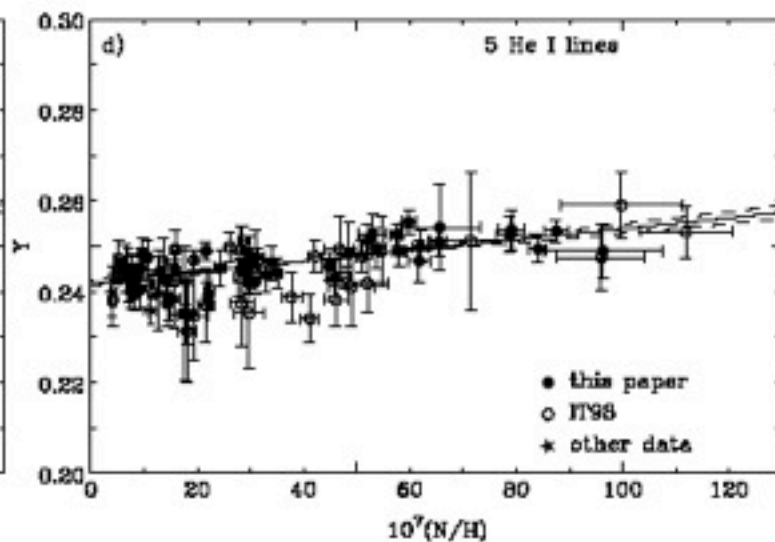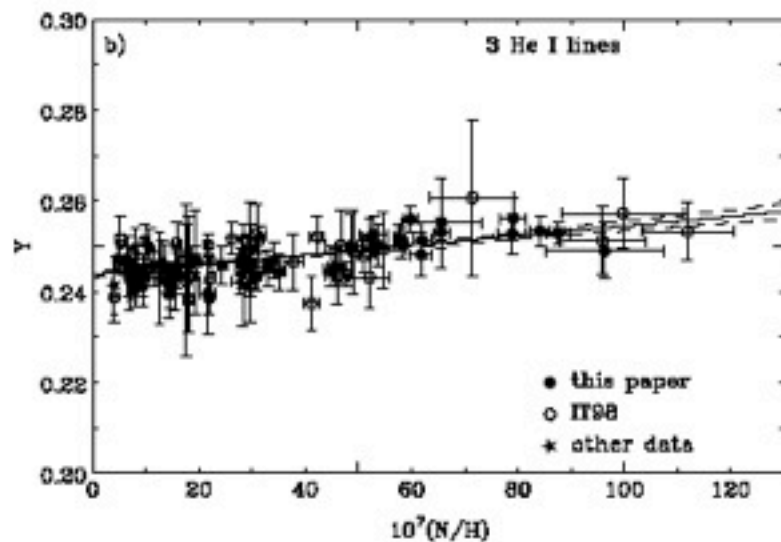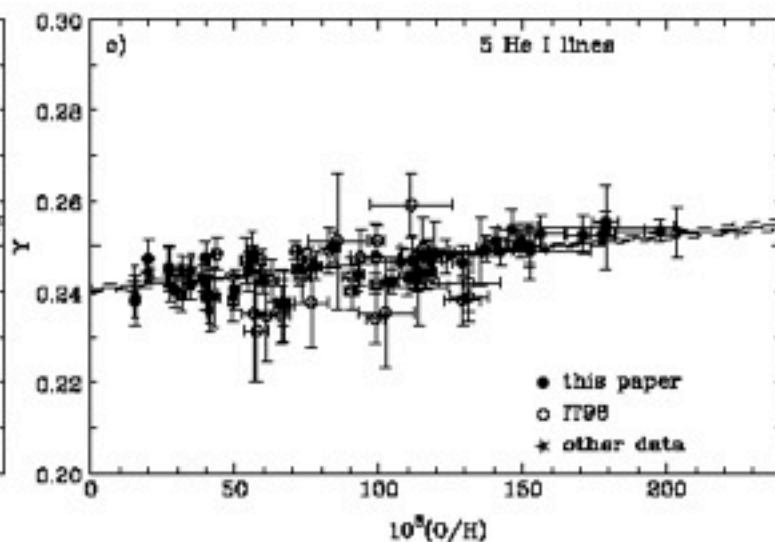
Ly-β   D   H
Ly-γ
Ly-4
Ly-5
Ly-6
Ly-7
Ly-8

Velocity (km sec⁻¹)

FIG. 7.— The HIRES spectrum of Ly-2 to 8, together with our model of the system, as given in Table 3.

Kirkman, Tytler, Suzuki, O'Meara, & Lubin 2004

Determination of primordial He[4] abundance Y_p by linear regression
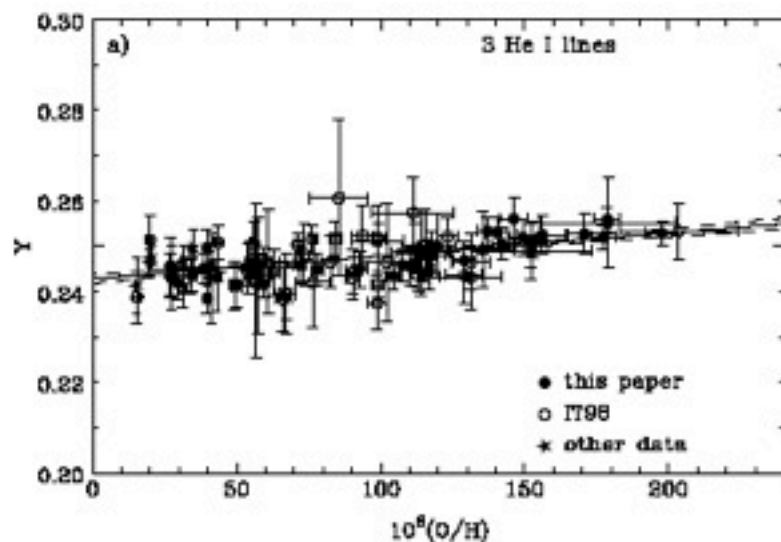
$Y = M(^4He)/M(baryons)$, Primordial $Y \equiv Yp$ = zero intercept

Note: BBN plus D/H $\Rightarrow$ Yp = 0.247$\pm$ 0.001

Izotov & Thuan 2004

The Li abundance disagreement with BBN may indicate new physics

Did Something Decay, Evaporate, or Annihilate during Big Bang Nucleosynthesis?

Karsten Jedamzik   Phys.Rev. D70 (2004) 063524

Laboratoire de Physique Mathémathique et Théorique, C.N.R.S.,
Université de Montpellier II, 34095 Montpellier Cedex 5, France

Results of a detailed examination of the cascade nucleosynthesis resulting from the putative hadronic decay, evaporation, or annihilation of a primordial relic during the Big Bang nucleosynthesis (BBN) era are presented. It is found that injection of energetic nucleons around cosmic time 10^3sec may lead to an observationally favored reduction of the primordial ^{7}Li/H yield by a factor $2-3$. Moreover, such sources also generically predict the production of the ^{6}Li isotope with magnitude close to the as yet unexplained high ^{6}Li abundances in low-metallicity stars. The simplest of these models operate at fractional contribution to the baryon density $\Omega_b h^2 \gtrsim 0.025$, slightly larger than that inferred from standard BBN. Though further study is required, such sources, as for example due to the decay of the next-to-lightest supersymmetric particle into GeV gravitinos or the decay of an unstable gravitino in the TeV range of abundance $\Omega_C h^2 \sim 5 \times 10^{-4}$ show promise to explain both the ^{6}Li and ^{7}Li abundances in low metallicity stars.

See also "Supergravity with a Gravitino LSP" by Jonathan L. Feng, Shufang Su, Fumihiro Takayama Phys.Rev. D70 (2004) 075019

"Gravitino Dark Matter and the Cosmic Lithium Abundances" by Sean Bailly, Karsten Jedamzik, Gilbert Moultaka, arXiv:0812.0788

The Li abundance disagreement with BBN may be caused by stellar diffusion
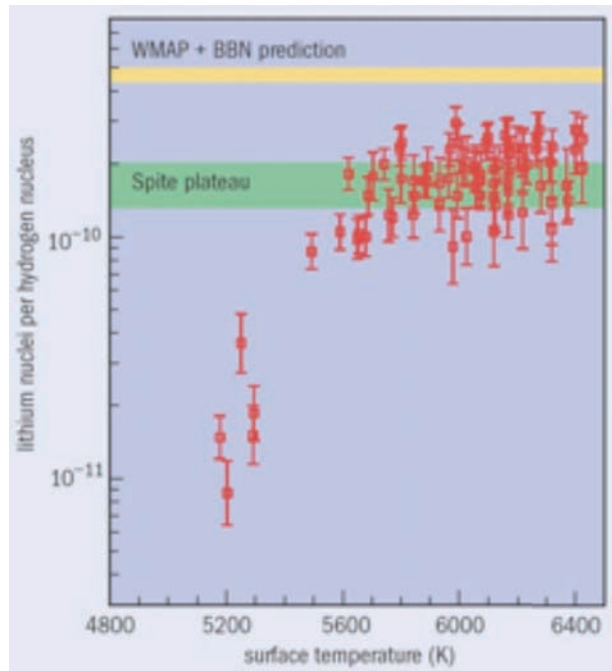
**Lithium abundance in very old stars that formed from nearly primordial gas.** The amount of ^{7}Li in these "Spite-plateau" stars (green) is much less than has been inferred by combining BBN with measurements of the cosmic microwave background made using WMAP (yellow band). Our understanding of stellar astrophysics may be at fault. Those Spite-plateau stars that have surface temperatures between 5700 and 6400 K have uniform abundances of ^{7}Li because the shallow convective envelopes of these warm stars do not penetrate to depths where the temperature exceeds that for ^{7}Li to be destroyed ($T_{destruct}$ =2.5 × 10^6 K). The envelopes of cooler stars (data points towards the left of the graph) do extend to such depths, so their surfaces have lost ^{7}Li to nuclear reactions. **If the warm stars gradually circulate ^{7}Li from the convective envelope to depths where T > T$_{destruct}$, then their surfaces may also slowly lose their ^{7}Li.** From http://physicsworld.com/cws/article/print/30680
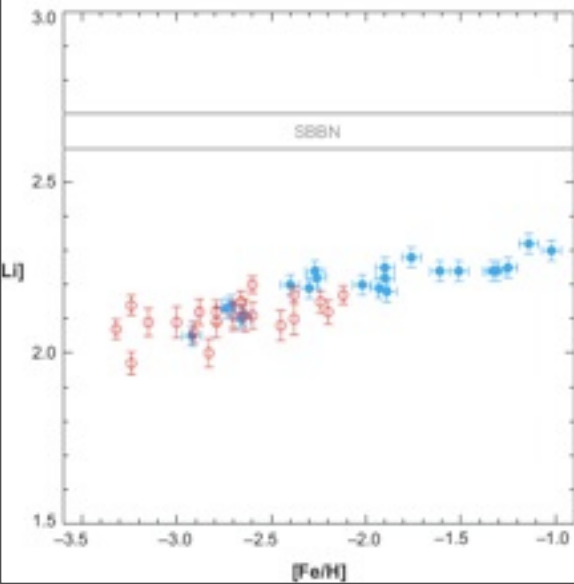
Lithium abundances, [Li] ≡ 12+ log(Li/H), versus metallicity (on a log scale relative to solar) from (red) S. Ryan et al. 2000, ApJ, 530, L57; (blue) M. Asplund et al.2006, ApJ, 644, 229. Figure from G. Steigman 2007, ARAA 57, 463.

Korn et al. 2006 find that both lithium and iron have settled out of the atmospheres of these old stars, and they infer for the unevolved abundances, [Fe/H] = –2.1 and [Li] = 2.54 ± 0.10, in excellent agreement with SBBN.

The most stringent constraint on a mixing model is that it must maintain the observed tight bunching of plateau stars that have the same average ^7Li abundance. In a series of papers that was published between 2002 and 2004, Olivier Richard and collaborators at the Université de Montréal in Canada proposed such a mixing model that has since gained observational support. It suggests that all nuclei heavier than hydrogen settle very slowly out of the convective envelope under the action of gravity. In particular, the model makes specific predictions for settling as a star evolves, which are revealed as variations of surface composition as a function of mass in stars that formed at the same time.

Korn et al. The Messenger 125 (Sept 2006); Korn et al. 2006, Nature 442, 657.
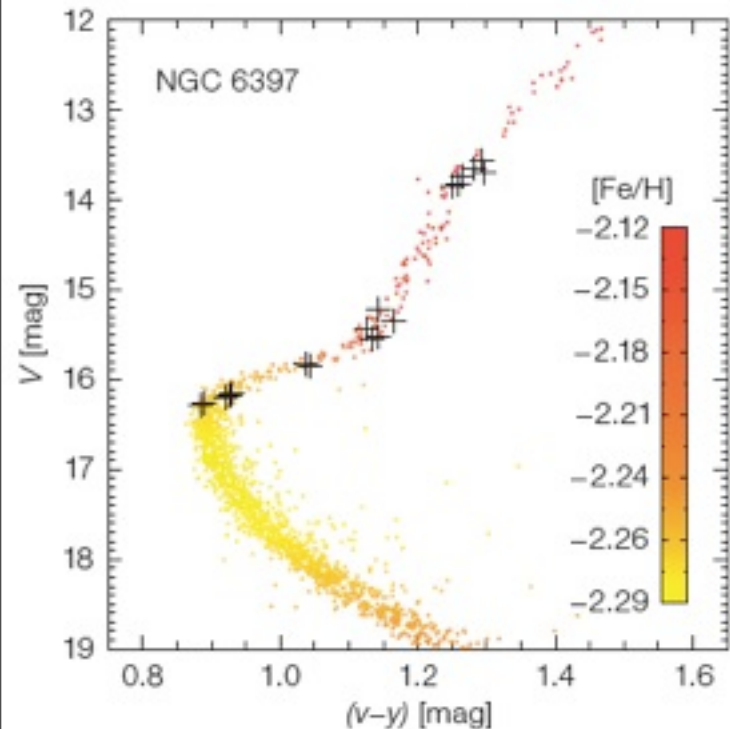
By spring 2006, Andreas Korn of Uppsala University in Sweden and colleagues had used the European Southern Observatory's Very Large Telescope (VLT) in Chile to study 18 chemically primitive stars in a distant globular cluster called NGC 6397 that were known to have the same age and initial composition. From this Korn et al. showed that the iron and lithium abundances in these stars both varied according to stellar mass as predicted by Richard's model. In fact, the model indicated that the observed stars started out with a ^7Li abundance that agrees with the WMAP data. Corroboration of these results is vital because **if the result stands up to scrutiny based on a wide range of data, then we have solved the lithium problem.**

A probable stellar solution to the cosmological lithium discrepancy A Korn et al.
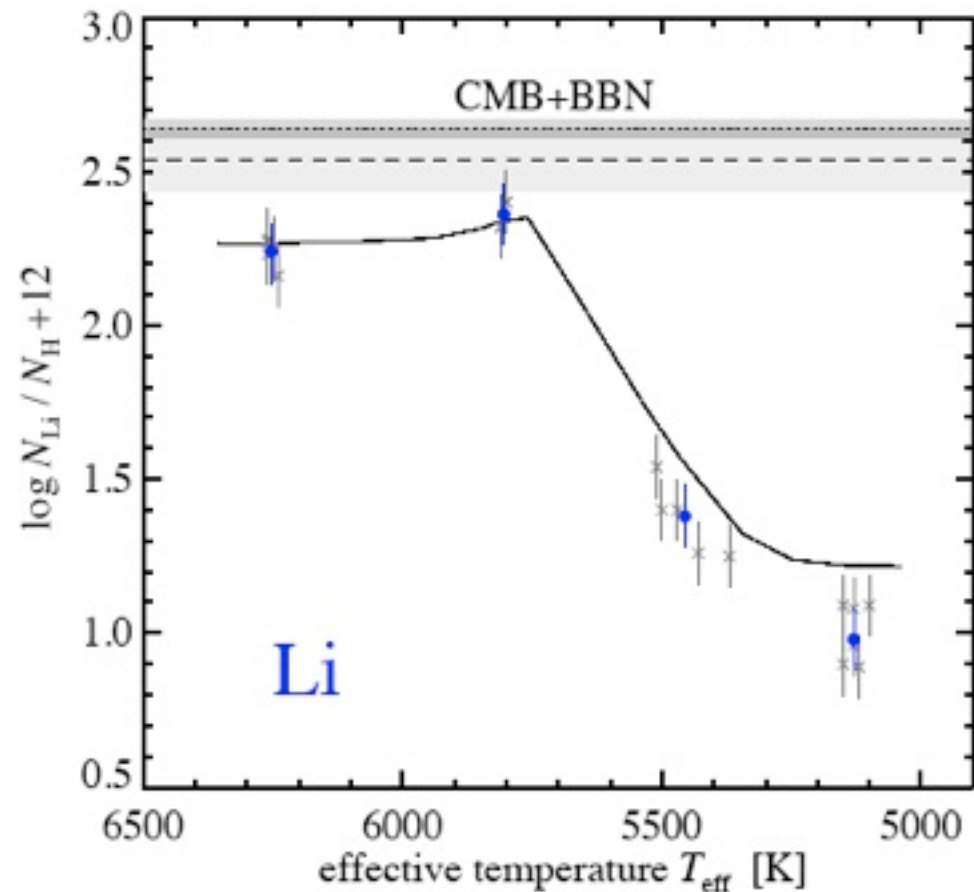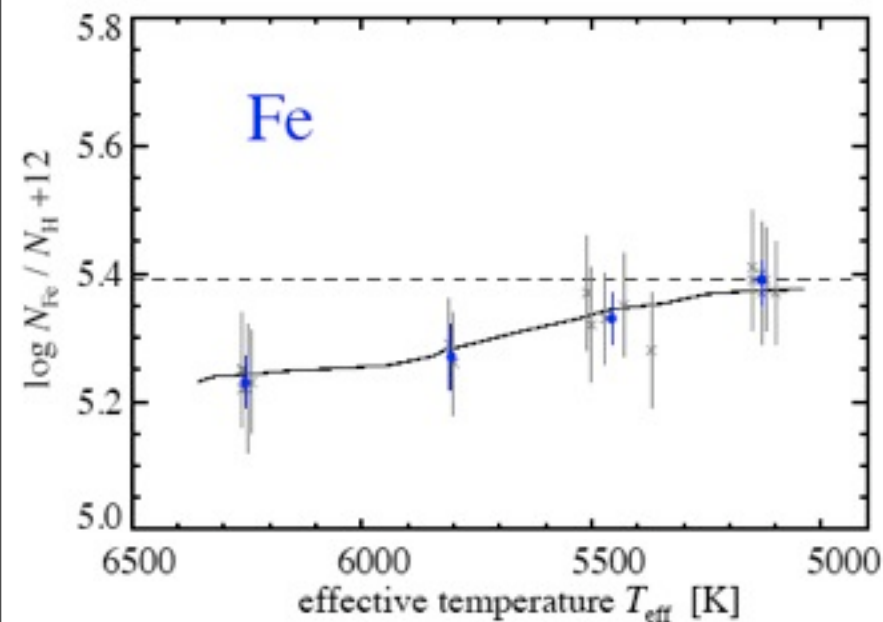
Figure 1: Trends of iron and lithium as a function of the effective temperatures of the observed stars compared to the model predictions. The grey crosses are the individual measurements, while the bullets are the group averages. The solid lines are the predictions of the diffusion model, with the original abundance given by the dashed line. In *b*, the grey-shaded area around the dotted line indicates the 1σ confidence interval of CMB + BBN[1]: $\log[\varepsilon(\text{Li})] = \log(N_{\text{Li}}/N_{\text{H}}) + 12 = 2.64 \pm 0.03$. In *a*, iron is treated in non-equilibrium[20] (non-LTE), while in *b*, the equilibrium (LTE) lithium abundances are plotted, because the combined effect of 3D and non-LTE corrections was found to be very small[29]. For iron, the error bars are the line-to-line scatter of Fe I and Fe II (propagated into the mean for the group averages), whereas for the absolute lithium abundances 0.10 is adopted. The 1σ confidence interval around the inferred primordial lithium abundance ($\log[\varepsilon(\text{Li})] = 2.54 \pm 0.10$) is indicated by the light-grey area. We attribute the modelling shortcomings with respect to lithium in the bRGB and RGB stars to the known need for extra mixing[30], which is not considered in the diffusion model.

Another way to determine the amount of ^{7}Li destroyed in stars is to observe the element's other, less stable, isotope: ^{6}Li. ^{6}Li is not made in detectable quantities by BBN but instead comes from spallation: collisions between nuclei in cosmic rays and in the interstellar gas. Since ^{6}Li is even more easily destroyed than ^{7}Li, detecting it allows us to place limits on the destruction of ^{7}Li.

In 2006 Martin Asplund and co-workers at the Mount Stromlo Observatory in Australia made extensive observations of ^{6}Li in plateau stars using the VLT. In each of the nine stars where they found ^{6}Li, roughly 5% of the lithium consisted of this isotope – which was larger than expected although at the limit of what was detectable with the equipment. This has huge implications not only for BBN but also for the history of cosmic rays in the galaxy and for stellar astrophysics. For example, the production of such large amounts of ^{6}Li must have required an enormous flux of cosmic rays early in the history of our galaxy, possibly more than could have been provided by known acceleration mechanisms. Moreover, if the plateau stars have truly destroyed enough ^{7}Li to bring the WMAP prediction of the mean baryon density into agreement with that obtained with the observed Spite plateau, the greater fragility of ^{6}Li implies that the stars initially contained ^{6}Li in quantities comparable to the observed ^{7}Li plateau.

All of these facts make the ^{6}Li observations an uncomfortable fit for BBN, stellar physics and models of cosmic-ray nucleosynthesis – particularly since the production of large amounts of ^{6}Li via cosmic rays has to be accompanied by a similar production of ^{7}Li. Although ^{6}Li can be produced in some exotic particle-physics scenarios, it is vital that we independently confirm Asplund's results. Indeed, the hunt for primordial lithium (of both isotopes) is currently ongoing at the VLT, as well as at the Keck Observatory and the Japanese Subaru Telescope, although such observations are right at the limit of what can be achieved.

Recent references on BBN and Lithium

M Asplund et al. 2006, "Lithium isotopic abundances in metalpoor halo stars" ApJ 644 229–259

T Beers and N Christlieb 2005, "The discovery and analysis of very metal-poor stars in the galaxy" Ann. Rev. Astron. Astrophys. 43, 531–580

A Korn et al. 2006 "A probable stellar solution to the cosmological lithium discrepancy" Nature 442, 657–659; 2007 "Atomic Diffusion and Mixing in Old Stars. I. Very Large Telescope FLAMES-UVES Observations of Stars in NGC 6397" ApJ 671, 402
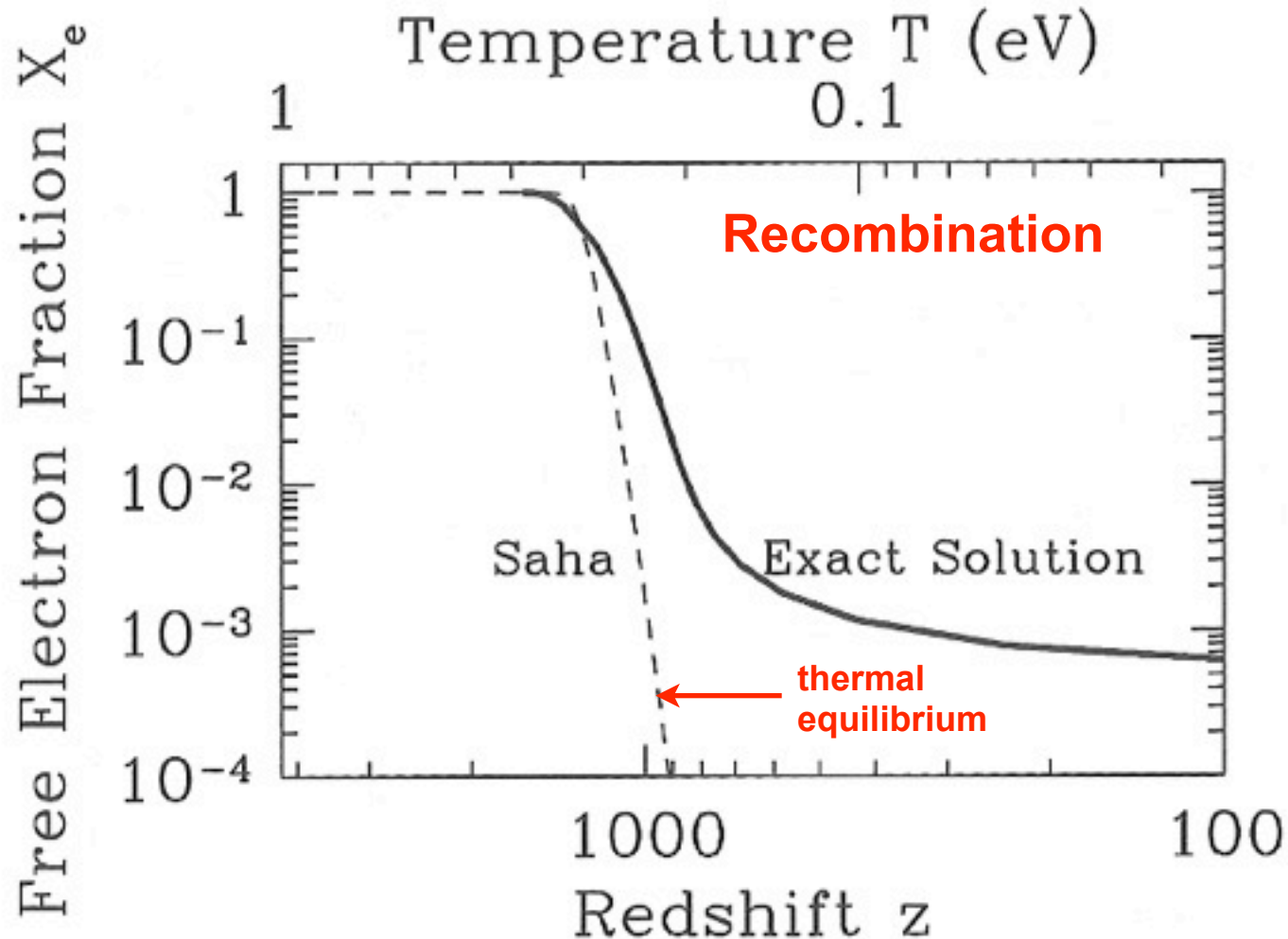
C Charbonnel 2006, "Where all the lithium went" Nature 442, 636-637
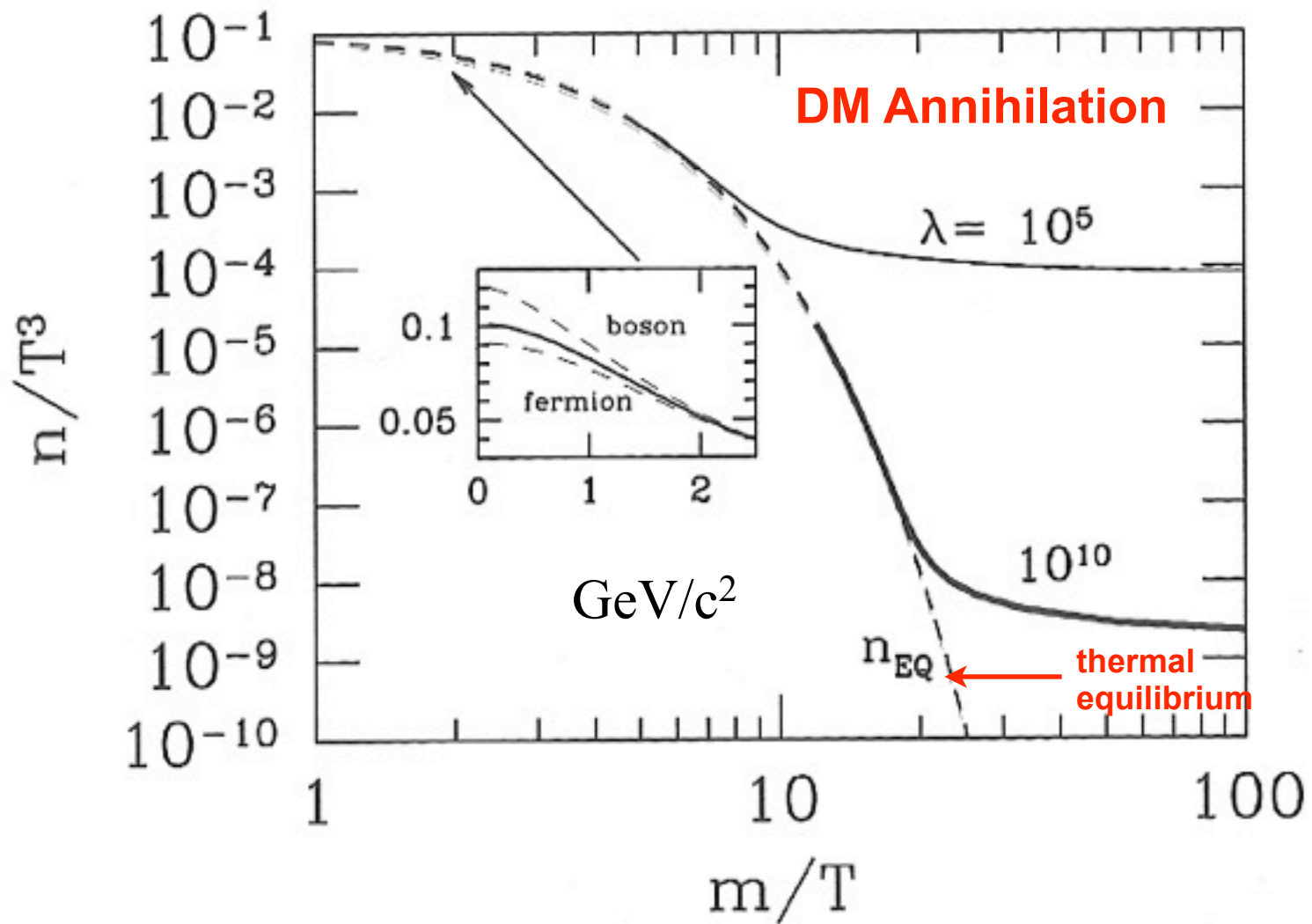
K Nollett 2007, "Testing the elements of the Big Bang" physicsworld.com

R H Cyburt, B D Fields, K A Olive 2008, "An update on the big bang nucleosynthesis prediction for 7Li: the problem worsens" JCAP 11, 12 (also arXiv:0808.2818)

A J Korn 2008 "Atomic Diffusion in Old Stars --- Helium, Lithium and Heavy Elements" ASPC 384, 33

BBN is a Prototype for Hydrogen Recombination and DM Annihilation

Figure 3.4. Free electron fraction as a function of redshift. Recombination takes place suddenly at $z \sim 1000$ corresponding to $T \sim 1/4$ eV. The Saha approximation, Eq. (3.37), holds in equilibrium and correctly identifies the redshift of recombination, but not the detailed evolution of X_e. Here $\Omega_b = 0.06$, $\Omega_m = 1$, $h = 0.5$.

Dodelson, *Modern Cosmology*, p. 72

Figure 3.5. Abundance of heavy stable particle as the temperature drops beneath its mass. Dashed line is equilibrium abundance. Two different solid curves show heavy particle abundance for two different values of λ, the ratio of the annihilation rate to the Hubble rate. Inset shows that the difference between quantum statistics and Boltzmann statistics is important only at temperatures larger than the mass.

Dodelson, *Modern Cosmology*, p. 76

In addition to the textbooks listed on the Syllabus for this course, a good place to find up-to-date information is the Particle Data Group website http://pdg.lbl.gov

For example, there are 2007 Mini-Reviews of

Big Bang Nucleosynthesis including a discussion of ^{7}Li
http://pdg.lbl.gov/2007/reviews/bigbangnucrpp.pdf

Big-Bang Cosmology
http://pdg.lbl.gov/2007/reviews/bigbangrpp.pdf

Cosmological Parameters
http://pdg.lbl.gov/2007/reviews/hubblerpp.pdf

CMB http://pdg.lbl.gov/2007/reviews/microwaverpp.pdf

and Dark Matter http://pdg.lbl.gov/2007/reviews/darkmatrpp.pdf
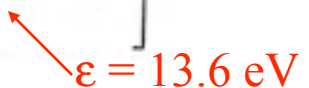
(Re)combination: e⁻ + p → H

As long as e- + p ⟺ H remains in equilibrium, the condition

$$\left\{ \frac{n_3 n_4}{n_3^{(0)} n_4^{(0)}} - \frac{n_1 n_2}{n_1^{(0)} n_2^{(0)}} \right\} = 0 \quad \text{with } 1 = e^-, 2 = p, 3 = H, \text{ ensures that} \quad \frac{n_e n_p}{n_H} = \frac{n_e^{(0)} n_p^{(0)}}{n_H^{(0)}}.$$

Neutrality ensures $n_p = n_e$. Defining the free electron fraction $X_e \equiv \dfrac{n_e}{n_e + n_H} = \dfrac{n_p}{n_p + n_H}$,

the equation above becomes $\dfrac{X_e^2}{1 - X_e} = \dfrac{1}{n_e + n_H} \left[\left(\dfrac{m_e T}{2\pi} \right)^{3/2} e^{-[m_e + m_p - m_H]/T} \right]$, which

$\varepsilon = 13.6$ eV

is known as the *Saha equation*. When T ~ **ε**, the rhs ~ 10^{15}, so X_e is very close to 1 and very little recombination has yet occurred. As T drops, the free electron fraction also drops, and as it approaches 0 equilibrium cannot be maintained. To follow the freezeout of the electron fraction, it is necessary to use the Boltzmann equation

$$a^{-3} \frac{d\left(n_e a^3\right)}{dt} = n_e^{(0)} n_p^{(0)} \langle \sigma v \rangle \left\{ \frac{n_H}{n_H^{(0)}} - \frac{n_e^2}{n_e^{(0)} n_p^{(0)}} \right\}$$

$$= n_b \langle \sigma v \rangle \left\{ (1 - X_e)\left(\frac{m_e T}{2\pi} \right)^{3/2} e^{-\epsilon_0/T} - X_e^2 n_b \right\}$$
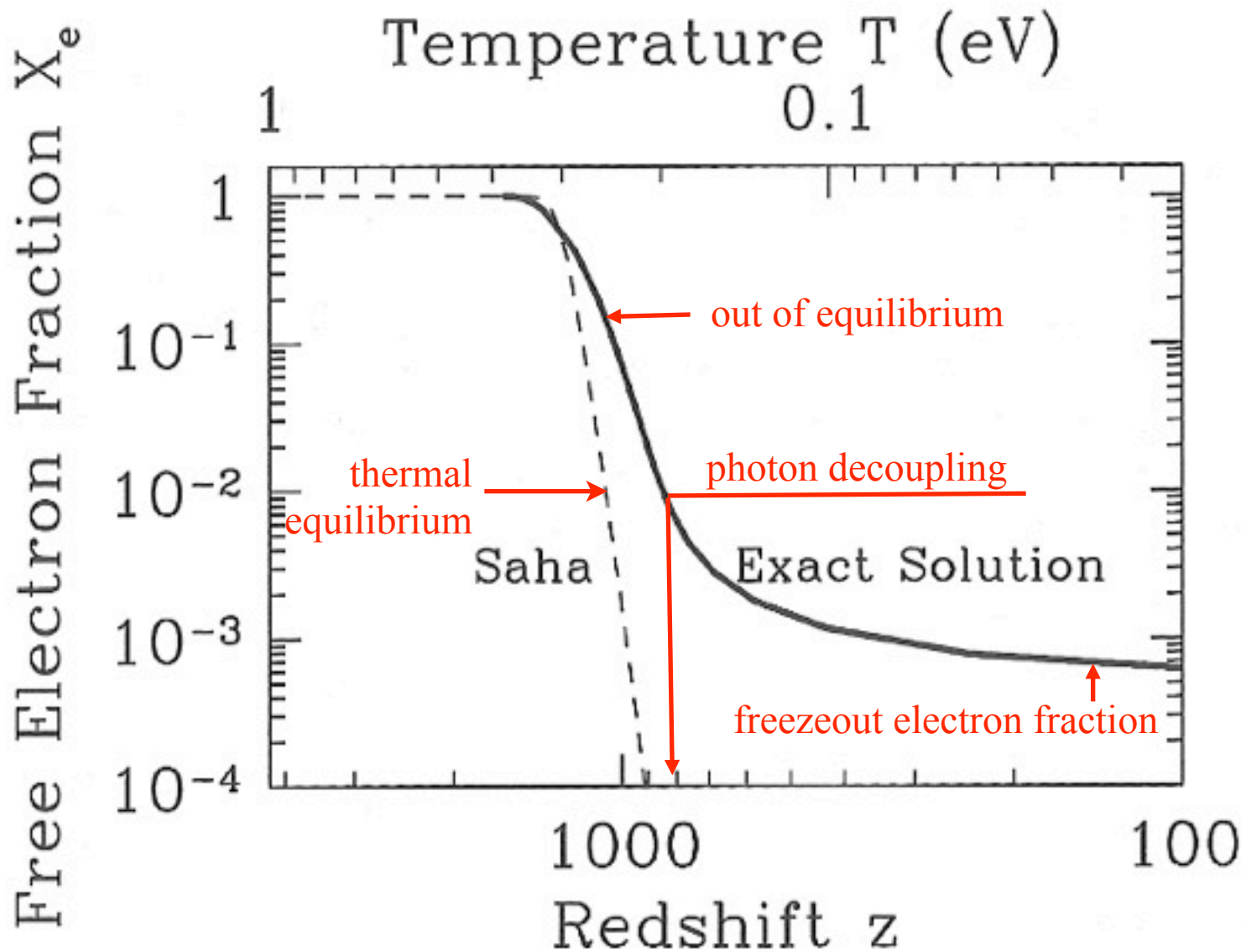
Figure 3.4. Free electron fraction as a function of redshift. Recombination takes place suddenly at $z \sim 1000$ corresponding to $T \sim 1/4$ eV. The Saha approximation, Eq. (3.37), holds in equilibrium and correctly identifies the redshift of recombination, but not the detailed evolution of X_e. Here $\Omega_b = 0.06$, $\Omega_m = 1$, $h = 0.5$.

Dodelson, *Modern Cosmology*, p. 72
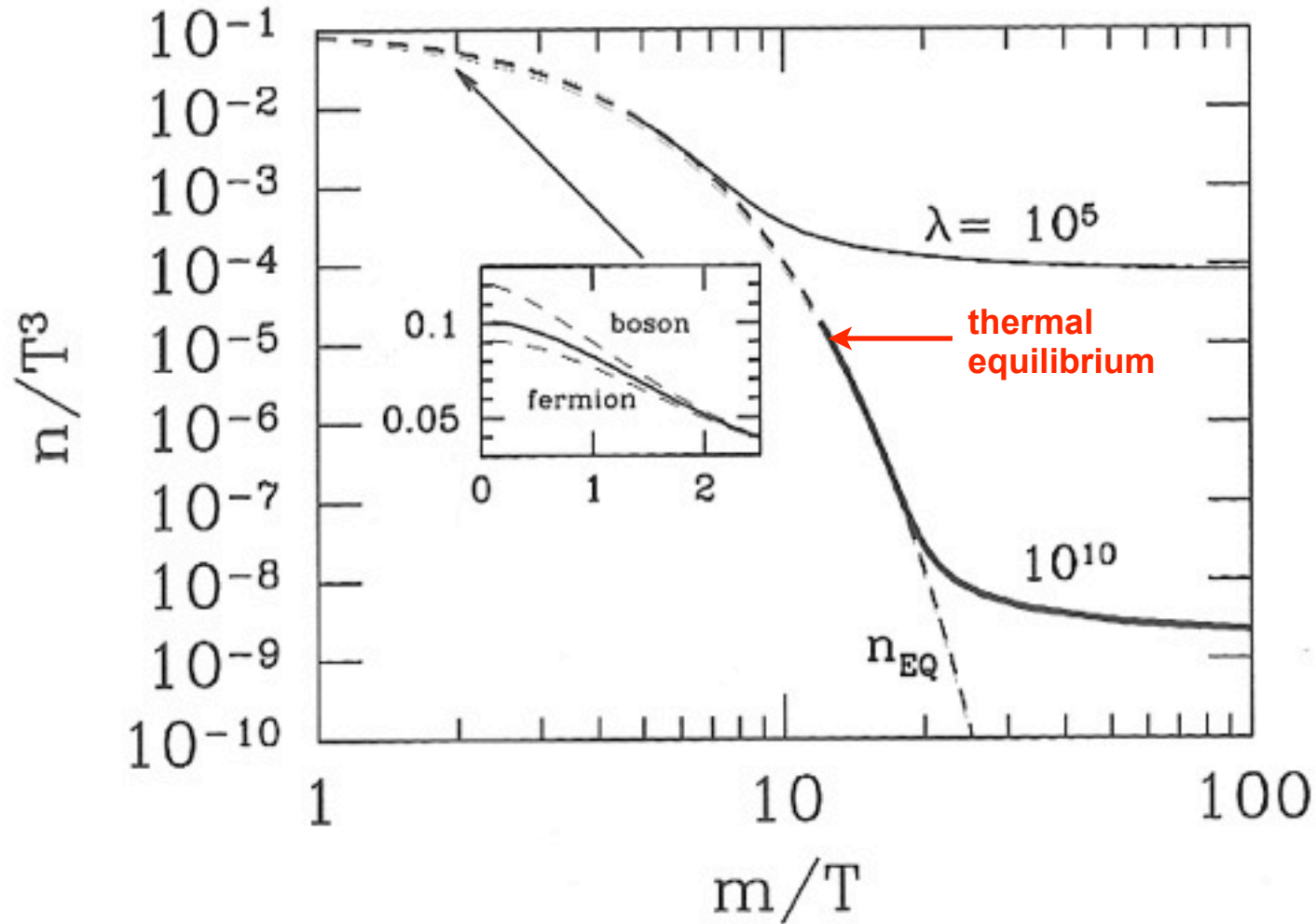
Dark Matter Annihilation

Figure 3.5. Abundance of heavy stable particle as the temperature drops beneath its mass. Dashed line is equilibrium abundance. Two different solid curves show heavy particle abundance for two different values of λ, the ratio of the annihilation rate to the Hubble rate. Inset shows that the difference between quantum statistics and Boltzmann statistics is important only at temperatures larger than the mass.

Dodelson, *Modern Cosmology*, p. 76

Dark Matter Annihilation

The weak shall inherit the universe!

thermal equilibrium

The weaker the cross section, the earlier freezeout occurs, and the larger the resulting dark matter density.
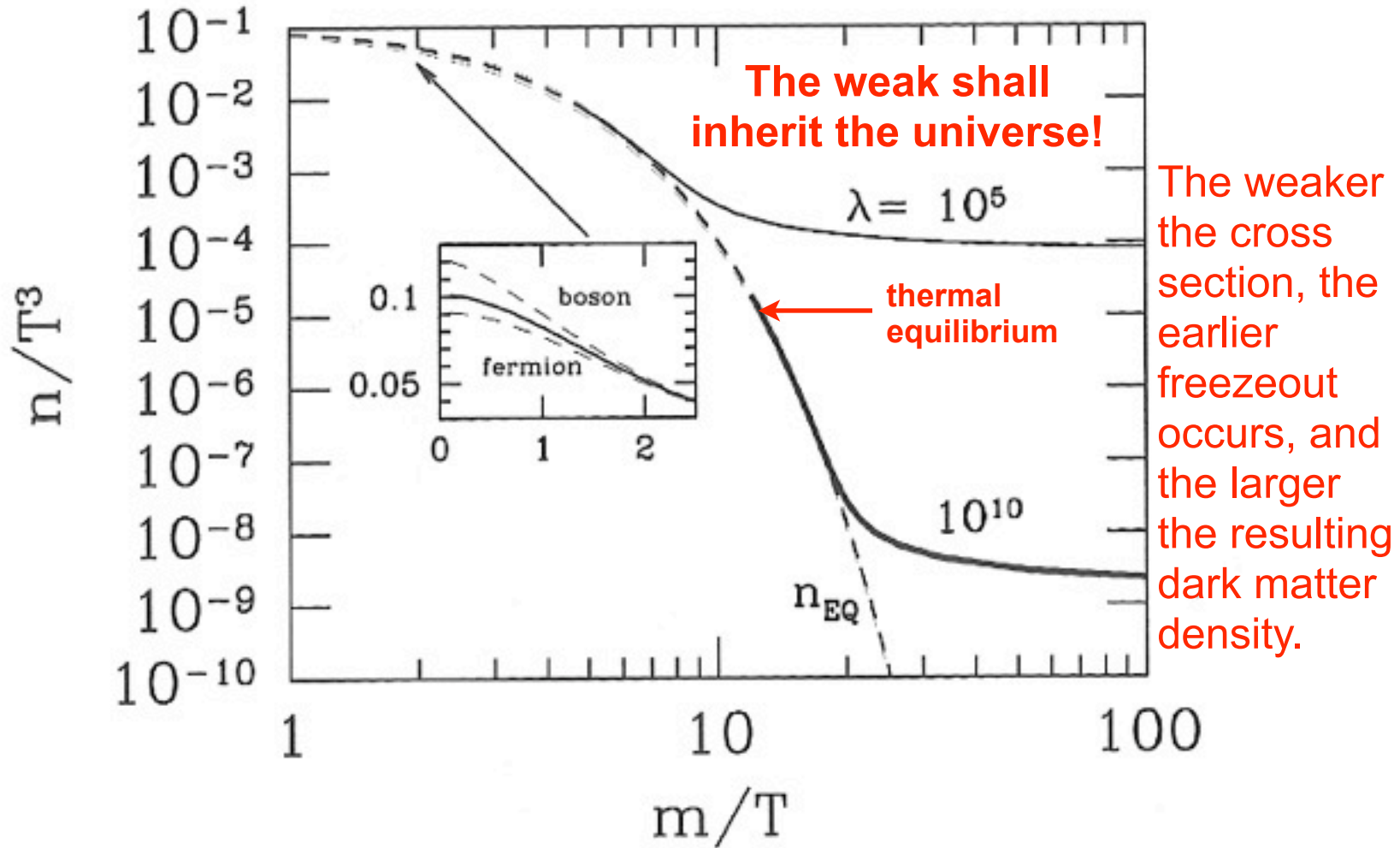
Figure 3.5. Abundance of heavy stable particle as the temperature drops beneath its mass. Dashed line is equilibrium abundance. Two different solid curves show heavy particle abundance for two different values of λ, the ratio of the annihilation rate to the Hubble rate. Inset shows that the difference between quantum statistics and Boltzmann statistics is important only at temperatures larger than the mass.

Dodelson, *Modern Cosmology*, p. 76

Dark Matter Annihilation

The abundance today of dark matter particles X of the WIMP variety is determined by their survival of annihilation in the early universe. Supersymmetric neutralinos can annihilate with each other (and sometimes with other particles: "co-annihilation"). Dark matter annihilation follows the same pattern as the previous discussions: initially the abundance of dark matter particles X is given by the equilibrium Boltzmann exponential $\exp(-m_X/T)$, but as they start to disappear they have trouble finding each other and eventually their number density freezes out. The freezeout process can be followed using the Boltzmann equation, as discussed in Kolb and Turner, Dodelson, Mukhanov, and other textbooks. For a detailed discussion of Susy WIMPs, see the review article by Jungman, Kamionkowski, and Griest (1996). The result is that the abundance today of WIMPs X is given in most cases by (Dodelson's Eqs. 3.59-60)

$$\Omega_X = \left[\frac{4\pi^3 G g_*(m)}{45}\right]^{1/2} \frac{x_f T_0^3}{30\langle\sigma v\rangle \rho_{cr}} = 0.3 h^{-2} \left(\frac{x_f}{10}\right) \left(\frac{g_*(m)}{100}\right)^{1/2} \frac{10^{-39} \text{cm}^2}{\langle\sigma v\rangle}.$$

Here $x_f \approx 10$ is the ratio of m_X to the freezeout temperature T_f, and $g_*(m_X) \approx 100$ is the density of states factor in the expression for the energy density of the universe when the temperature equals m_X

$$\rho = \frac{\pi^2}{30} T^4 \left[\sum_{i=\text{bosons}} g_i + \frac{7}{8} \sum_{i=\text{fermions}} g_i\right] \equiv g_* \frac{\pi^2}{30} T^4.$$

The sum is over relativistic species i (see the graph of $g(T)$ on the next slide). Note that more X's survive, the weaker the cross section σ. For Susy WIMPs the natural values are $\sigma \sim 10^{-39}$ cm^2, so $\Omega_X \approx 1$ naturally.
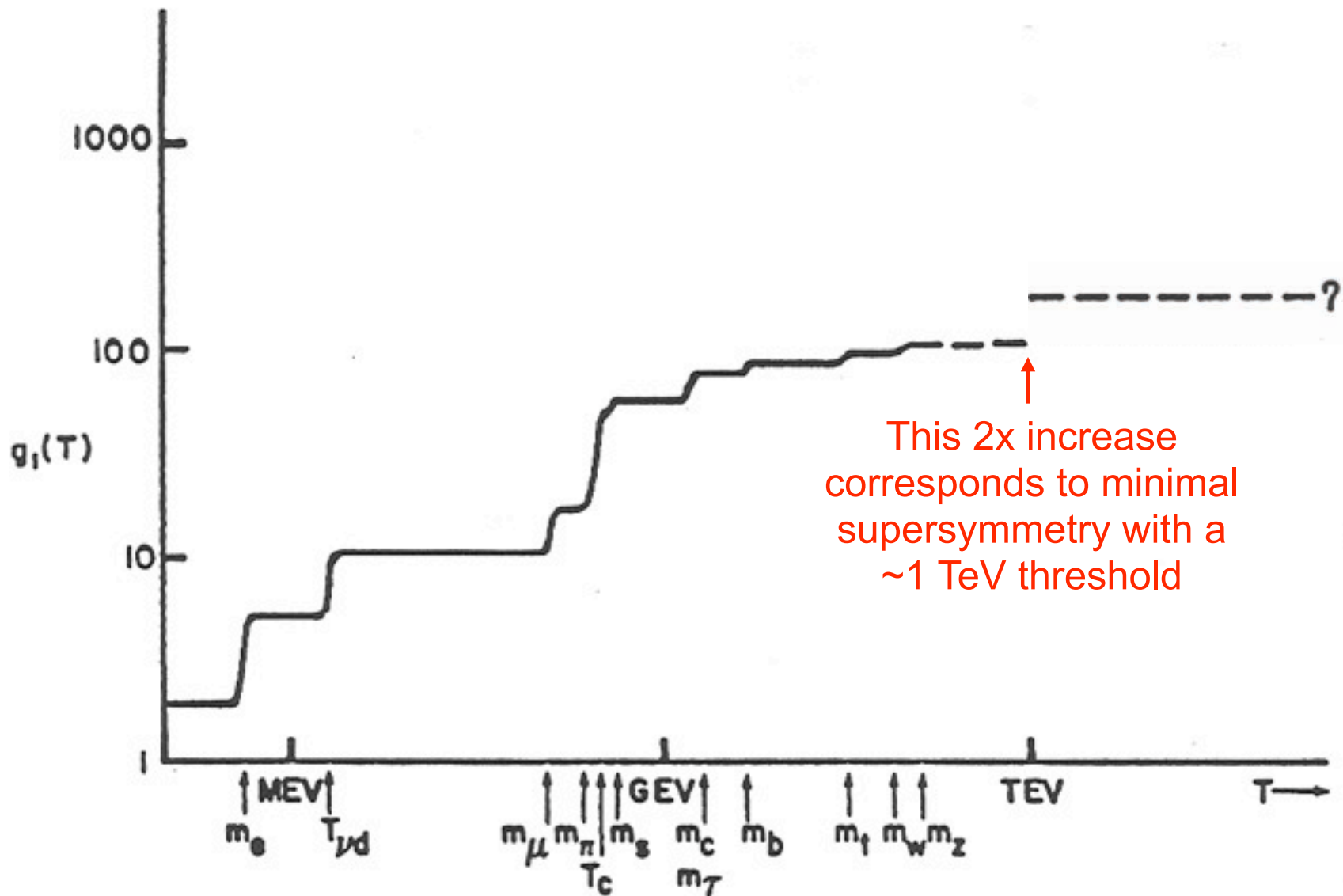
Fig. 1 The effective number of degrees of freedom of thermally interacting relativistic particles as a function of temperature.

Supersymmetry is the basis of most attempts, such as superstring theory, to go beyond the current "Standard Model" of particle physics. Heinz Pagels and Joel Primack pointed out in a 1982 paper that the lightest supersymmetric partner particle is stable because of R-parity, and is thus a good candidate for the dark matter particles – weakly interacting massive particles (**WIMP**s).

Michael Dine and others pointed out that the **axion**, a particle needed to save the strong interactions from violating CP symmetry, could also be the dark matter particle. Searches for both are underway.

Supersymmetric WIMPs

When the British physicist Paul Dirac first combined Special Relativity with quantum mechanics, he found that this predicted that for every ordinary particle like the electron, there must be another particle with the opposite electric charge – the anti-electron (positron). Similarly, corresponding to the proton there must be an anti-proton. Supersymmetry appears to be required to combine General Relativity (our modern theory of space, time, and gravity) with the other forces of nature (the electromagnetic, weak, and strong interactions). The consequence is another doubling of the number of particles, since supersymmetry predicts that for every particle that we now know, including the antiparticles, there must be another, thus far undiscovered particle with the same electric charge but with *spin* differing by half a unit.

Spin	Matter (fermions)	Forces (bosons)
2		graviton
1		photon, $W^{\pm}, Z^0$ gluons
1/2	quarks u,d,... leptons $e, \nu_e, \ldots$	
0		Higgs bosons axion

underlined.

Supersymmetric WIMPs

When the British physicist Paul Dirac first combined Special Relativity with quantum mechanics, he found that this predicted that for every ordinary particle like the electron, there must be another particle with the opposite electric charge – the anti-electron (positron). Similarly, corresponding to the proton there must be an anti-proton. Supersymmetry appears to be required to combine General Relativity (our modern theory of space, time, and gravity) with the other forces of nature (the electromagnetic, weak, and strong interactions). The consequence is another doubling of the number of particles, since supersymmetry predicts that for every particle that we now know, including the antiparticles, there must be another, thus far undiscovered particle with the same electric charge but with *spin* differing by half a unit.

after doubling

Spin	Matter (fermions)	Forces (bosons)	Hypothetical Superpartners	Spin
2		graviton	gravitino	3/2
1		photon, $W^\pm, Z^0$ gluons	photino, winos, zino, gluinos	1/2
1/2	quarks u,d,... leptons $e, \nu_e, \ldots$		squarks $\tilde{u}, \tilde{d}, \ldots$ sleptons $\tilde{e}, \tilde{\nu}_e, \ldots$	0
0		Higgs bosons axion	Higgsinos axinos	1/2

Note: Supersymmetric cold dark matter candidate particles are underlined.

Supersymmetric WIMPs, continued

Spin is a fundamental property of elementary particles. Matter particles like electrons and quarks (protons and neutrons are each made up of three quarks) have spin ½, while force particles like photons, W,Z, and gluons have spin 1. The supersymmetric partners of electrons and quarks are called selectrons and squarks, and they have spin 0. The supersymmetric partners of the force particles are called the photino, Winos, Zino, and gluinos, and they have spin ½, so they might be matter particles. The lightest of these particles might be the photino. Whichever is lightest should be stable, so it is a natural candidate to be the dark matter WIMP. Supersymmetry does not predict its mass, but it must be more than 50 times as massive as the proton since it has not yet been produced at accelerators. But it will be produced soon at the LHC, if it exists and its mass is not above ~1 TeV!

SUPERSYMMETRY

The only experimental evidence for supersymmetry is that running of coupling constants in the Standard Model does not lead to Grand Unification (of the weak, electromagnetic, and strong interactions)
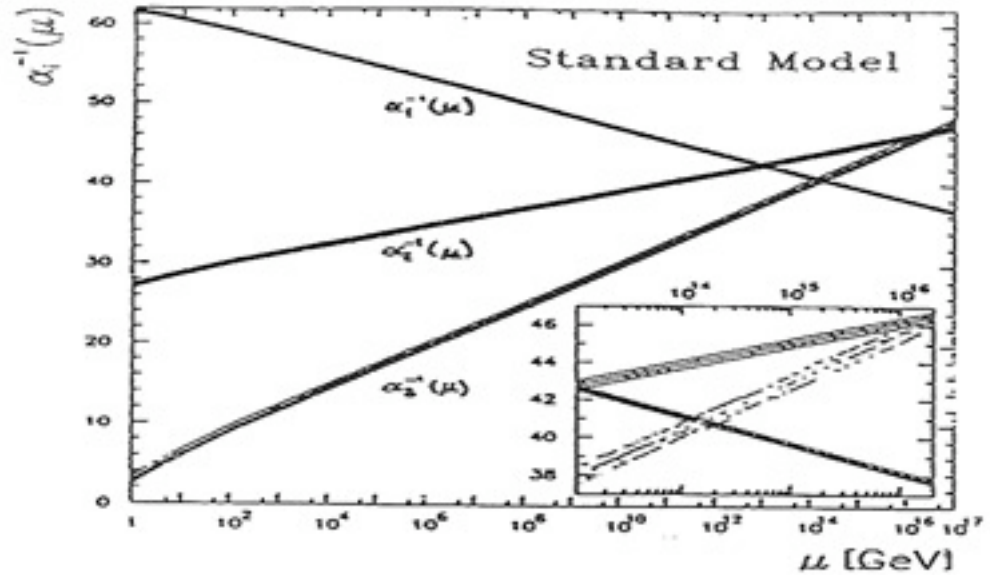

while with supersymmetry the three couplings all do come together at a scale just above 10^{16} GeV.

Other arguments for SUSY include: helps unification of gravity since it controls the vacuum energy and moderates loop divergences, solves the hierarchy problem, and naturally leads to DM with $\Omega \approx 1$.
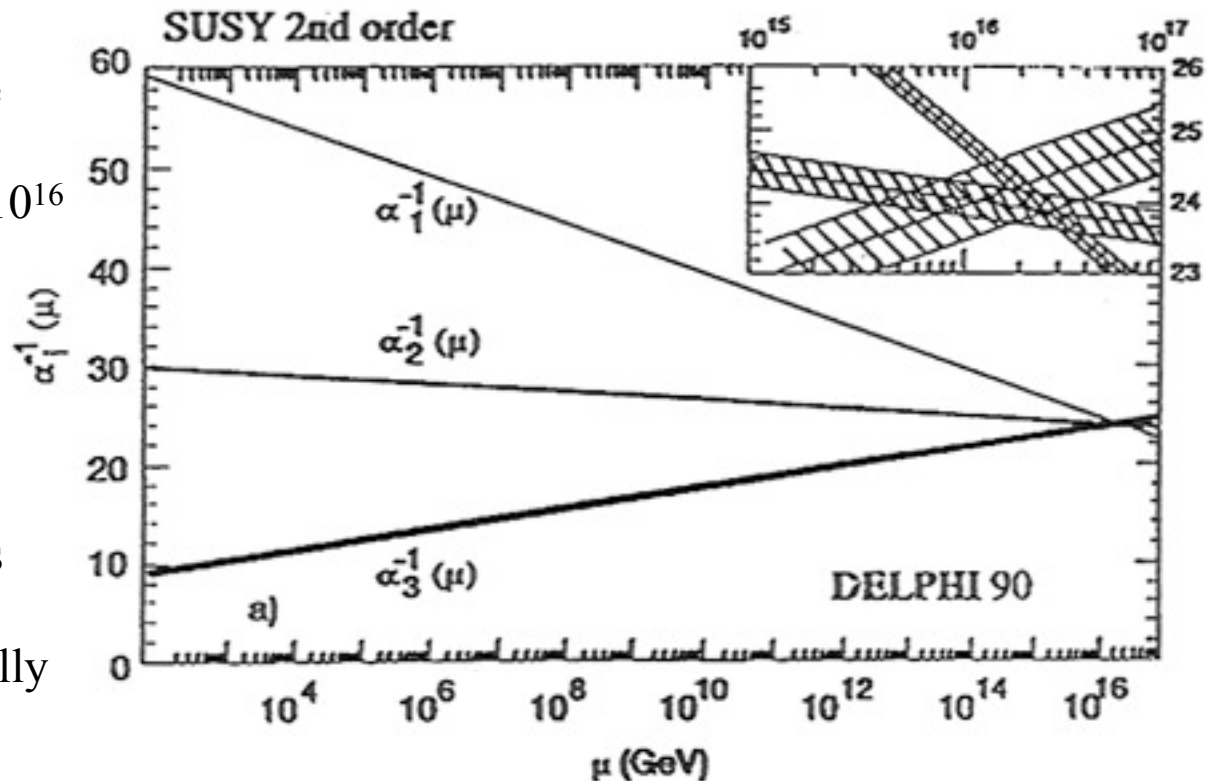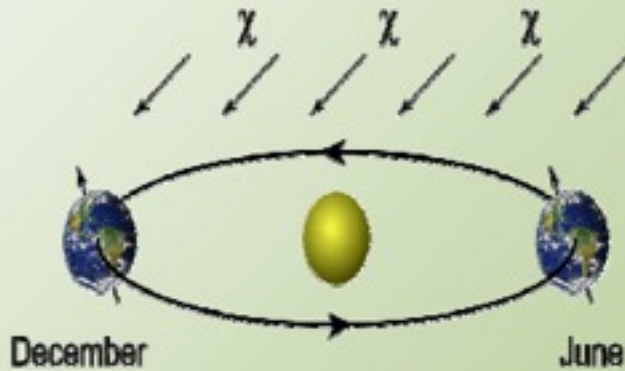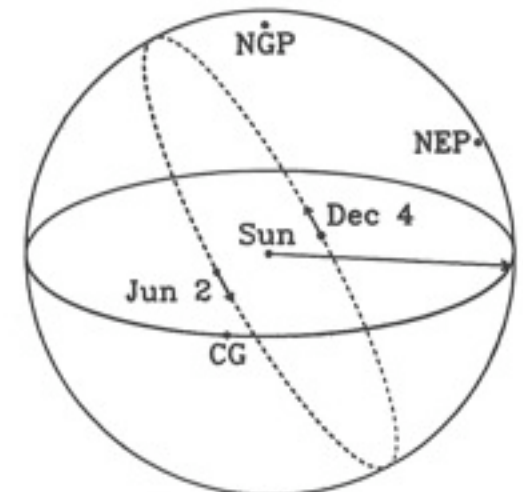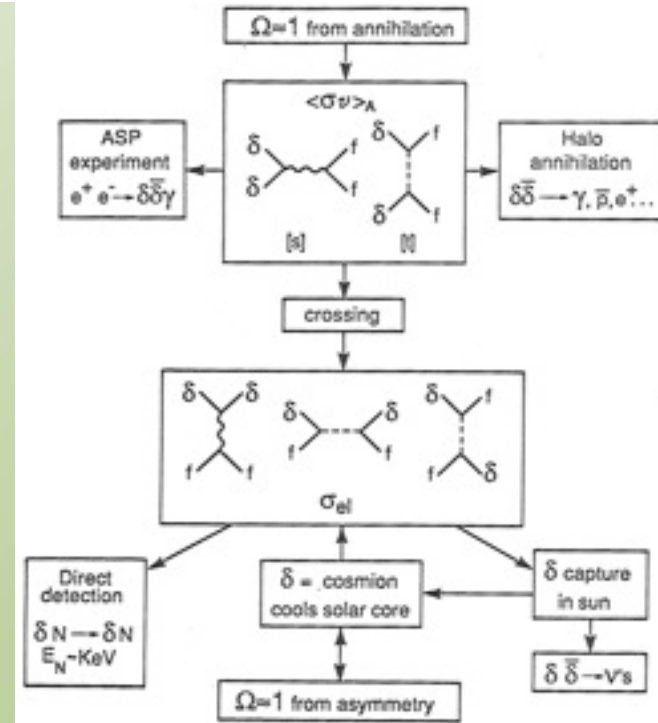
Experiments are Underway for Detection of WIMPs

Direct detection - general principles
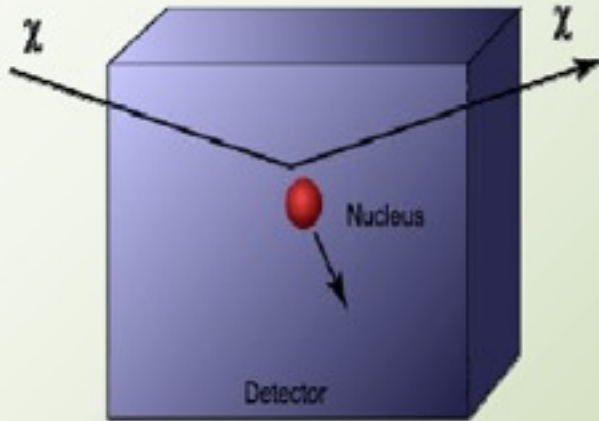
- WIMP + nucleus →
  WIMP + nucleus

- Measure the nuclear recoil
  energy

- Suppress backgrounds enough
  to be sensitive to a signal, or...

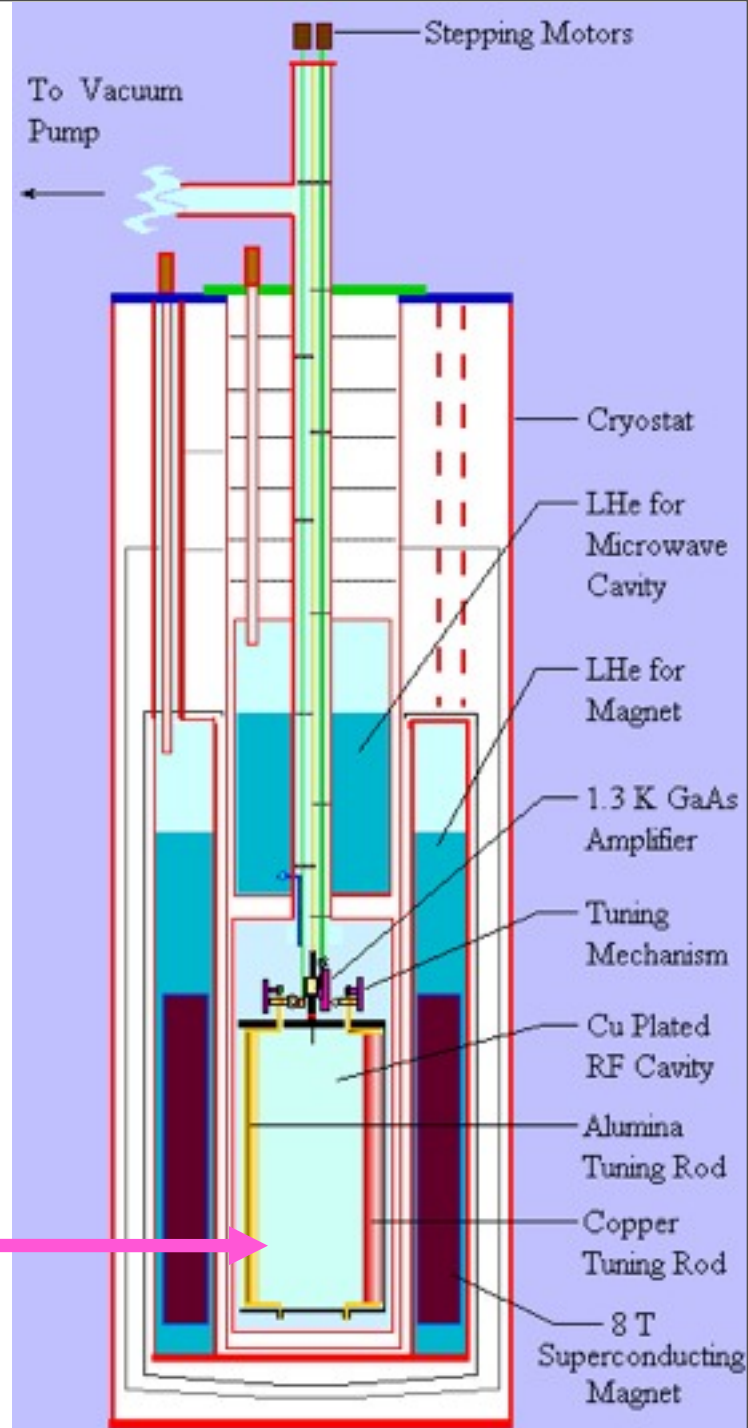- Search for an annual
  modulation due to the Earth's
  motion around the Sun

Primack, Seckel, & Sadoulet (1987)

and also AXIONs

The diagram at right shows the layout of the axion search experiment now underway at the Lawrence Livermore National Laboratory. Axions would be detected as extra photons in the Microwave Cavity.

Types of Dark Matter

Ω_i represents the fraction of the critical density $\rho_c = 10.54 \, h^2 \, \text{keV/cm}^3$ needed to close the Universe, where h is the Hubble constant H_0 divided by 100 km/s/Mpc.

Dark Matter Type	Fraction of Critical Density	Comment
Baryonic	$\Omega_b \sim 0.04$	about 10 times the visible matter
Hot	$\Omega_v \sim 0.001 - 0.1$	light neutrinos
Cold	$\Omega_c \sim 0.3$	most of the dark matter in galaxy halos

Dark Matter and Associated Cosmological Models

Ω_m represents the fraction of the critical density in all types of matter.
Ω_Λ is the fraction contributed by some form of "dark energy."

Acronym	Cosmological Model	Flourished
HDM	hot dark matter with $\Omega_m = 1$	1978–1984
SCDM	standard cold dark matter with $\Omega_m = 1$	1982–1992
CHDM	cold + hot dark matter with $\Omega_c \sim 0.7$ and $\Omega_v = 0.2-0.3$	1994–1998
ΛCDM	cold dark matter $\Omega_c \sim 1/3$ and $\Omega_\Lambda \sim 2/3$	1996–today

THE ATMOSPHERIC-NEUTRINO DATA from the Super-Kamiokande underground neutrino detector in Japan provide strong evidence of muon to tau neutrino oscillations, and therefore that these neutrinos have nonzero mass (see the article by John Learned in the Winter 1999 *Beam Line*, Vol. 29, No. 3). This result is now being confirmed by results from the K2K experiment, in which a muon neutrino beam from the KEK accelerator is directed toward Super-Kamiokande and the number of muon neutrinos detected is about as expected from the atmospheric-neutrino data (see article by Jeffrey Wilkes and Koichiro Nishikawa, this issue).

But oscillation experiments cannot measure neutrino masses directly, only the squared mass difference $\Delta m_{ij}^2 = |m_i^2 - m_j^2|$ between the oscillating species. The Super-Kamiokande atmospheric neutrino data imply that $1.7 \times 10^{-4} < \Delta m_{\tau\mu}^2 < 4 \times 10^{-3}$ eV² (90 percent confidence), with a central value $\Delta m_{\tau\mu}^2 = 2.5 \times 10^{-3}$ eV². If the neutrinos have a hierarchical mass pattern $m_{\nu_e} \ll m_{\nu_\mu} \ll m_{\nu_\tau}$ like the quarks and charged leptons, then this implies that $\Delta m_{\tau\mu}^2 \cong m_{\nu_\tau}^2$ so $m_{\nu_\tau} \sim 0.05$ eV.

These data then imply a lower limit on the HDM (or light neutrino) contribution to the cosmological matter density of $\Omega_\nu > 0.001$—almost as much as that of all the stars in the disks of galaxies. There is a connection between neutrino mass and the corresponding contribution to the cosmological density, because the thermodynamics of the early Universe specifies the abundance of neutrinos to be about 112 per cubic centimeter for each of the three species (including both neutrinos and antineutrinos). It follows that the density Ω_ν contributed by neutrinos is $\Omega_\nu = m(\nu)/(93\,h^2$ eV), where $m(\nu)$ is the sum of the masses of all three neutrinos. Since $h^2 \sim 0.5$, $m_{\nu_\tau} \sim 0.05$ eV corresponds to $\Omega_\nu \sim 10^{-3}$.

This is however a lower limit, since in the alternative case where the oscillating neutrino species have nearly equal masses, the values of the individual masses could be much larger. The only other laboratory approaches to measuring neutrino masses are attempts to detect neutrino-less double beta decay, which are sensitive to a possible Majorana component of the electron neutrino mass, and measurements of the endpoint of the tritium beta-decay spectrum. The latter gives an upper limit on the electron neutrino mass, currently taken to be 3 eV. Because of the small values of both squared-mass differences, this tritium limit becomes an upper limit on all three neutrino masses, corresponding to $m(\nu) < 9$ eV. A bit surprisingly, cosmology already provides a stronger constraint on neutrino mass than laboratory measurements, based on the effects of neutrinos on large-scale structure formation.

Joel Primack, *Beam Line*, Fall 2001

fermion masses

(large angle MSW)

Hitoshi Murayama
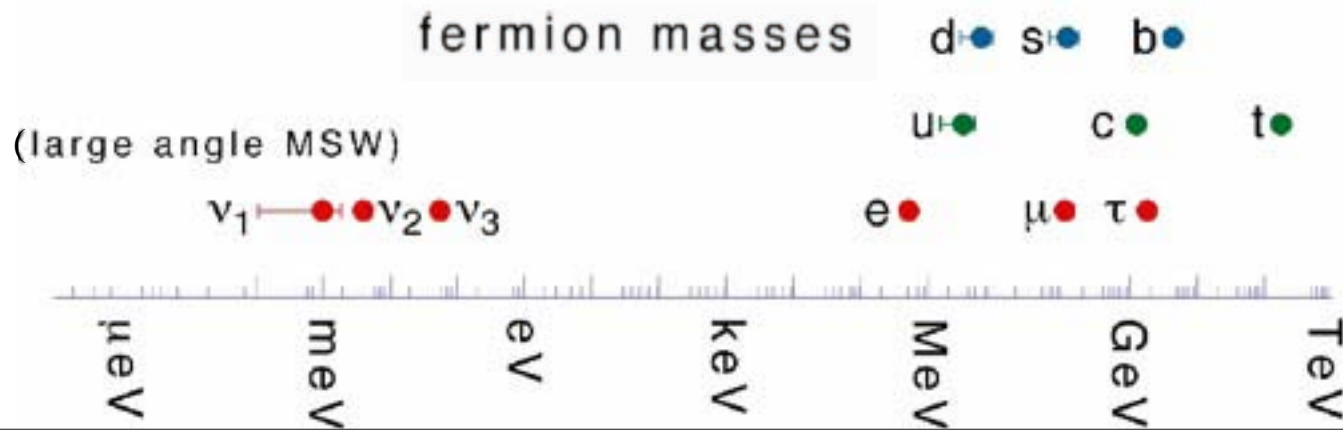
Neutrino Properties

See the note on "Neutrino properties listings" in the Particle Listings.

Mass $m < 2$ eV (tritium decay)

Mean life/mass, $\tau/m > 300$ s/eV, CL = 90% (reactor)

Mean life/mass, $\tau/m > 7 \times 10^9$ s/eV (solar)

Mean life/mass, $\tau/m > 15.4$ s/eV, CL = 90% (accelerator)

Magnetic moment $\mu < 0.9 \times 10^{-10}\ \mu_B$, CL = 90% (reactor)

Number of Neutrino Types

Number $N = 2.994 \pm 0.012$ (Standard Model fits to LEP data)

Number $N = 2.93 \pm 0.05$ (S = 1.2) (Direct measurement of invisible Z width)

Neutrino Mixing

The following values are obtained through data analyses based on the 3-neutrino mixing scheme described in the review "Neutrino mass, mixing, and flavor change" by B. Kayser in this *Review*.

$$\sin^2(2\theta_{12}) = 0.86^{+0.03}_{-0.04}$$

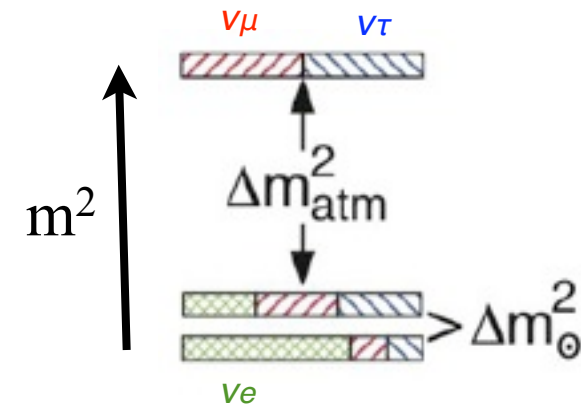$$\Delta m^2_{21} = (8.0^{+0.4}_{-0.3}) \times 10^{-5}\ \text{eV}^2$$

The ranges below for $\sin^2(2\theta_{23})$ and Δm^2_{32} correspond to the projections onto the appropriate axes of the 90% CL contours in the $\sin^2(2\theta_{23})$-Δm^2_{32} plane.

$$\sin^2(2\theta_{23}) > 0.92$$

$$\Delta m^2_{32} = 1.9 \text{ to } 3.0 \times 10^{-3}\ \text{eV}^2\ [i]$$

$$\sin^2(2\theta_{13}) < 0.19,\ \text{CL} = 90\%$$

A three-neutrino squared-mass spectrum that accounts for the observed flavor changes of solar, reactor, atmospheric, and long-baseline accelerator neutrinos. The ν_e fraction of each mass eigenstate is crosshatched, the ν_μ fraction is indicated by right-leaning hatching, and the ν_τ fraction by left-leaning hatching. From B. Kaiser, http://pdg.lbl.gov/2007/reviews/

numixrpp.pdf

Sudbury Neutrino Observatory Confirms Solar Neutrinos Oscillate

$n \rightarrow p\, e^-\, \bar{\nu}_e$ must happen twice per ^{4}He, and then ~1/3 of the electron antineutrinos oscillate to mu or tau neutrinos
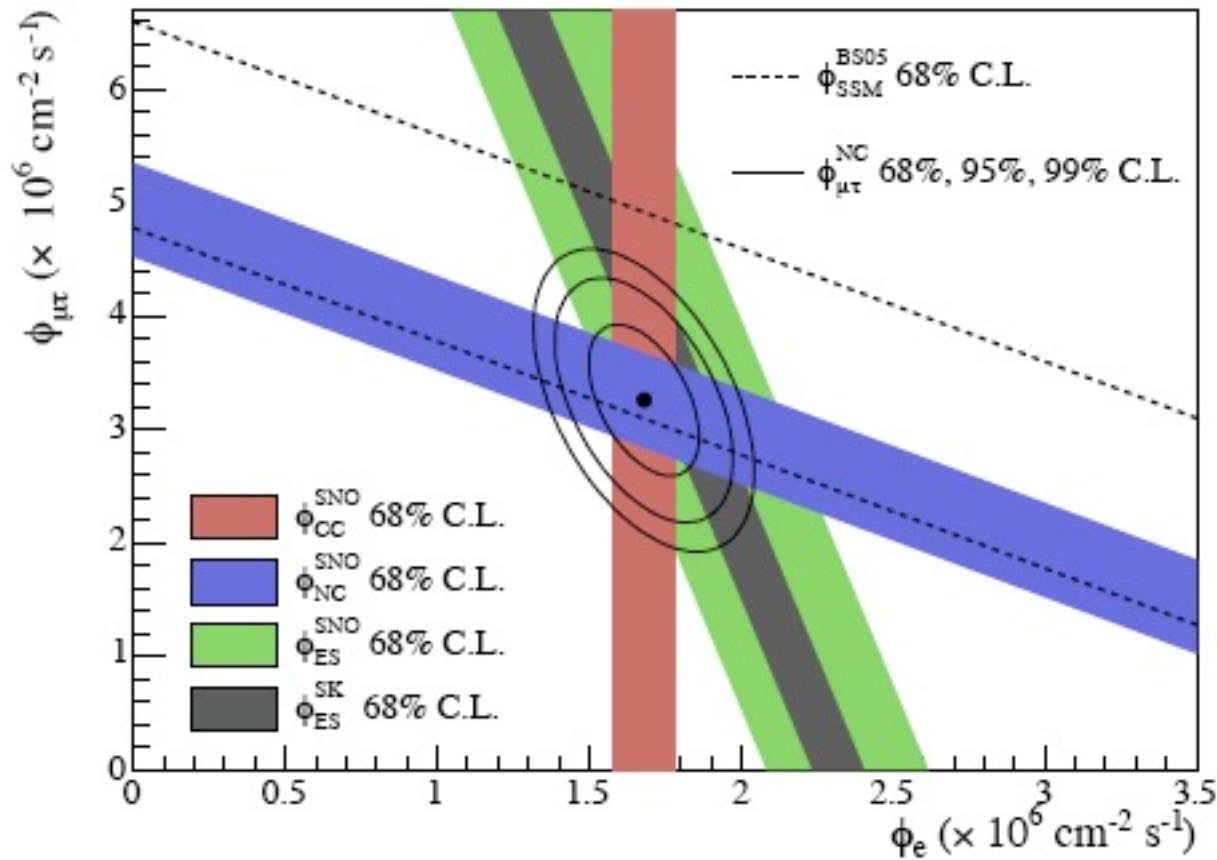
Fluxes of ^{8}B solar neutrinos, $\phi(\nu_e)$, and $\phi(\nu_\mu \text{ or } \tau)$, deduced from the SNO's charged current (CC), ν_e elastic scattering (ES), and neutral-current (NC) results for the salt phase measurement. The Super-Kamiokande ES flux and the BS05(OP) standard solar model prediction are also shown. The bands represent the 1σ error. The contours show the 68%, 95%, and 99% joint probability for $\phi(\nu_e)$ and $\phi(\nu_\mu \text{ or } \tau)$.

[From PDG 2005 review by K. Nakamura.]
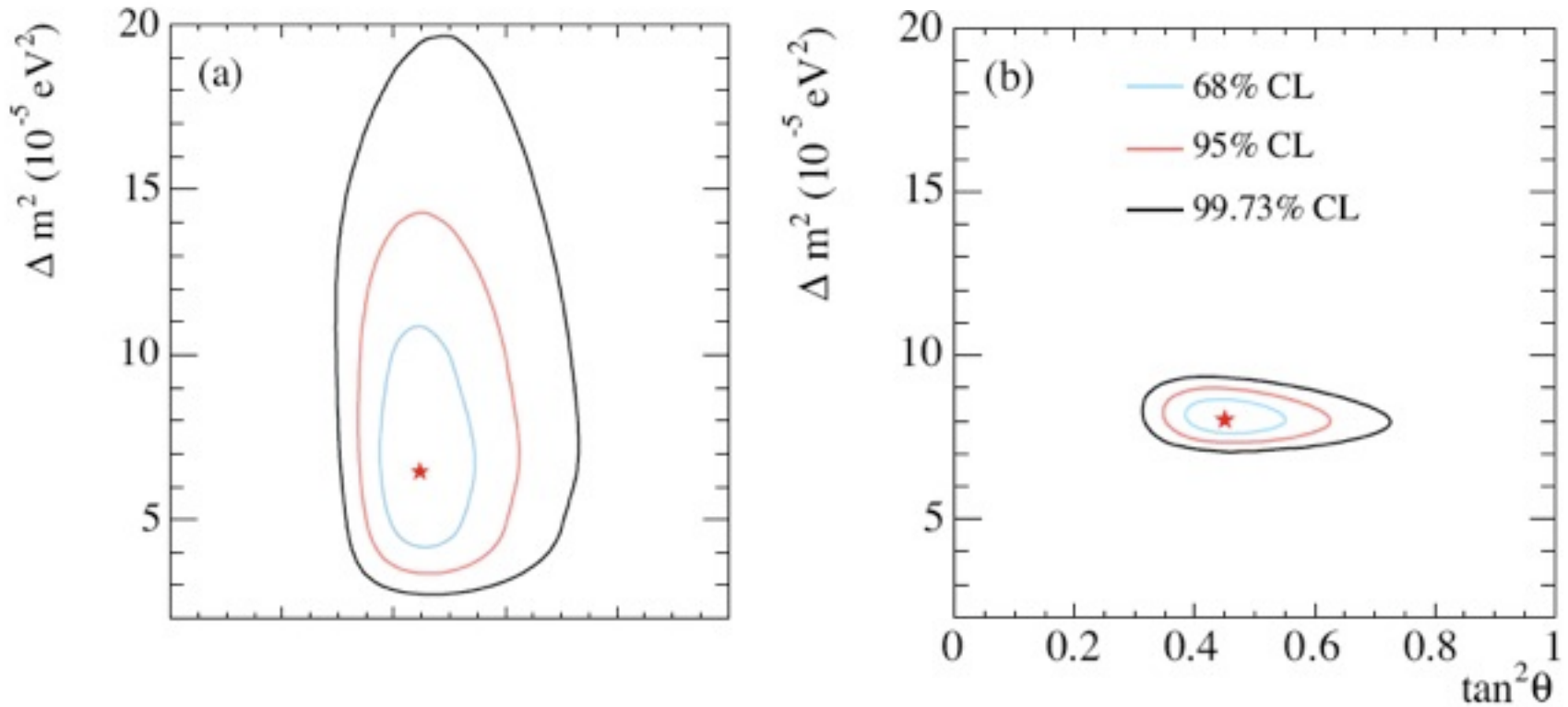
Update of the global neutrino oscillation contours given by the SNO Collaboration assuming that the ^{8}B neutrino flux is free and the *hep* neutrino flux is fixed. (a) Solar global analysis. (b) Solar global + KamLAND. [From PDG 2005 review by K. Nakamura.]

$$\Delta m_{12}^2 = 8 \times 10^{-5} \text{ eV}^2 \Rightarrow m_2 \geq 9 \times 10^{-3} \text{ eV}$$
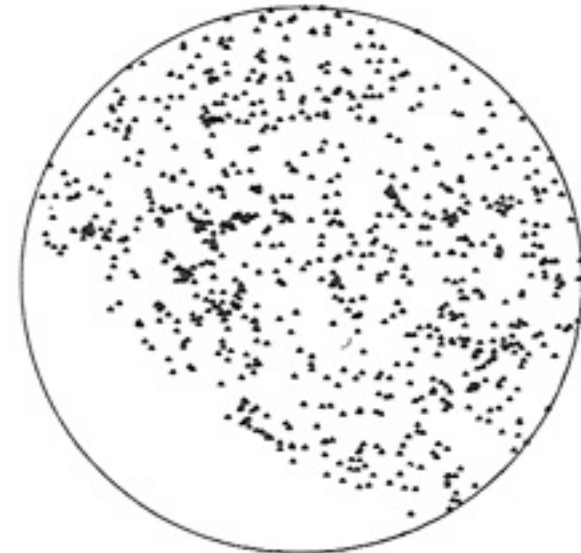
Whatever Happened to Hot Dark Matter?

In ~1980, when purely baryonic adiabatic fluctuations were ruled out by the improving upper limits on CMB anisotropies, theorists led by Zel'dovich turned to what we now call the HDM scenario, with light neutrinos making up most of the dark matter. However, in this scheme the fluctuations on small scales are damped by relativistic motion ("free streaming") of the neutrinos until T becomes less than m_ν, which occurs when the mass entering the horizon is about 10^{15} solar masses, the supercluster mass scale. Thus superclusters would form first, and galaxies later by fragmentation. This predicted a galaxy distribution much more inhomogeneous than observed.
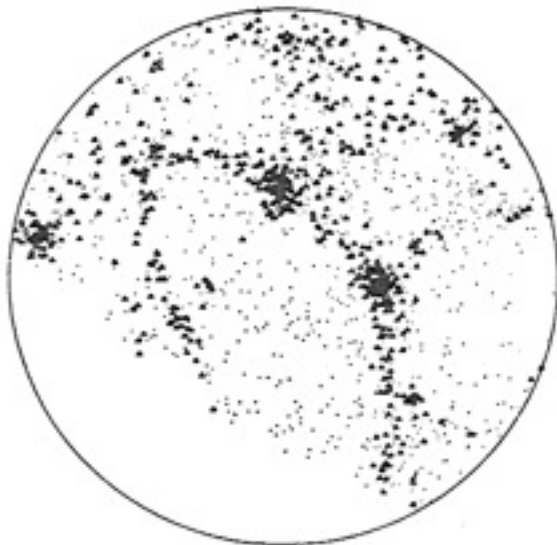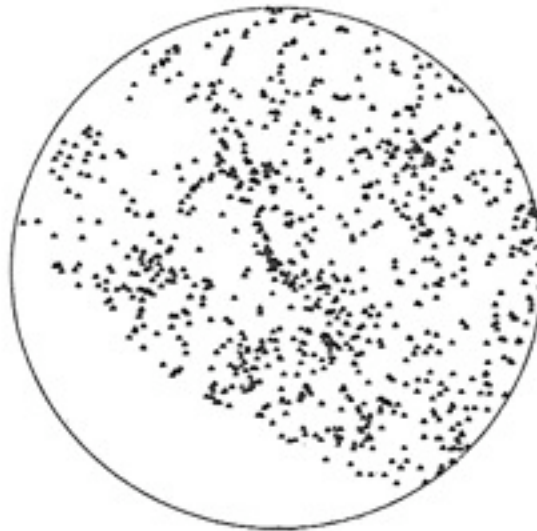
HDM   Observed Galaxy Distribution   CDM

Since 1984, the most successful structure formation scenarios have been those in which most of the matter is CDM. With the COBE CMB data in 1992, two CDM variants appeared to be viable: ΛCDM with $\Omega_m \approx 0.3$, and $\Omega_m = 1$ Cold+Hot DM with $\Omega_v \approx 0.2$. A potential problem with CHDM was that, like all $\Omega_m = 1$ theories, it predicted rather late structure formation. A potential problem with ΛCDM was that the correlation function of the dark matter was higher around 1 Mpc than the power-law $\xi_{gg}(r) = (r/r_0)^{-1.8}$ observed for galaxies, so "scale-dependent anti-biasing" was required (Klypin, Primack, & Holtzman 1996, Jenkins et al. 1998). When better ΛCDM simulations could resolve halos that could host galaxies, they were found to have the same correlations as observed for galaxies.

By 1998, the evidence of early galaxy and cluster formation and the increasing evidence that $\Omega_m \approx 0.3$ had doomed CHDM. But now we also know from neutrino oscillations that neutrinos have mass. The upper limit from cosmology is $\Omega_v h^2 < 0.002$, corresponding to $m_v < 0.17$ eV (95% CL) for the most massive neutrino (Seljak et al. 2006).